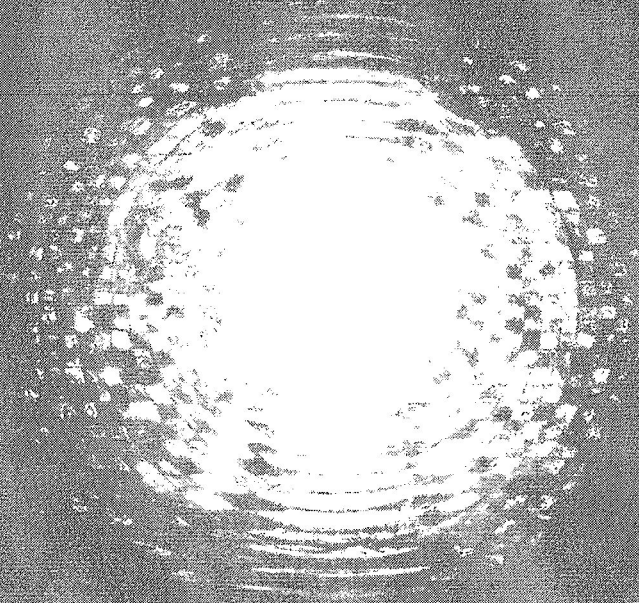


① N 70 27513

# LTV RESEARCH CENTER

FINAL REPORT  
 CONTRACT NAS8-30521  
 INVESTIGATIONS OF  
 ELECTRON INTERACTIONS IN MATTER  
 Report No. O-71100/OR-6  
 March 1970

CASE FILE  
COPY



007-64009



FINAL REPORT  
CONTRACT NAS8-30521  
INVESTIGATIONS OF  
ELECTRON INTERACTIONS IN MATTER

Report No. O-71100/OR-6

March 1970

Prepared by:

*D. H. Rester*

D. H. Rester  
Senior Scientist

Approved by:

*Jim Howard Johnson*

J. H. Johnson - Manager  
Nuclear and Space Physics

*H. B. Gibbons*

H. B. Gibbons  
Director

FINAL REPORT

CONTRACT NO. NAS8-30521

Period Covering March 12, 1969 through March 12, 1970

COMPARISONS OF EXPERIMENTAL AND CALCULATED ELECTRON TRANSMISSION  
AND BREMSSTRAHLUNG SPECTRA FOR ELECTRON ENERGIES BELOW 3.0 MEV

by David H. Rester

LTV RESEARCH CENTER

Report No. 0-71100/OR-6

March 1970

Prepared for George C. Marshall Space Flight Center,  
Huntsville, Alabama,  
by LTV Research Center  
Nuclear and Space Physics Group  
Dallas, Texas

## TABLE OF CONTENTS

	<u>Page No.</u>
I. Introduction .....	1
II. Thick Target Bremsstrahlung .....	2
III. Electron Transmission of Thick Targets .....	6
IV. Bremsstrahlung Cross Sections .....	9
V. Appendix .....	11
VI. References .....	13
VII. Figures .....	14

## INTRODUCTION

Thick-target bremsstrahlung measurements have been reported for a number of elements in the electron energy range of 0.2 to 2.8 MeV. Related electron diffusion experiments have also been reported in the same energy range. Although these experiments were performed primarily for comparison to calculations, only a limited number of the experimental spectra have been compared to calculated spectra.

In the present report numerous comparisons of the experimental results published earlier are made to the thick-target bremsstrahlung and electron diffusion spectra generated by the Monte Carlo program ETRAN 15 of M. J. Berger and S. M. Seltzer of the National Bureau of Standards. The spectra were calculated at the George C. Marshall Space Flight Center, NASA, by J. H. Derrickson.

In addition to comparisons of thick-target bremsstrahlung and electron transmission spectra, several comparisons of experimental electron bremsstrahlung cross-section values to theoretical values from the relativistic, self-consistent field model of Brysk, Zerby and Penny are included. Because of the complexity of the theory, it was practical to evaluate the formulas only in a restricted electron energy range. Evaluations of the formulas of Brysk, Zerby, and Penny were carried out at the George C. Marshall Space Flight Center, NASA. Modifications of the original programs were made by Q. Peasley, who supplied the values shown in this report.

## THICK-TARGET BREMSSTRAHLUNG

Experimental studies of electron bremsstrahlung have been reported at incident electron energies of 0.2, 1.0, 2.0, and 2.8 MeV for Al, Fe, Sn, and Au targets and at electron energies of 0.2, 1.0, and 2.0 MeV for Be targets.<sup>1</sup> For these measurements the electron beam was directed to the targets with perpendicular incidence. Limited thick-target bremsstrahlung measurements have also been made for the case of non-perpendicular incidence of the electron beam to the target.<sup>2</sup> Comparisons included in this section, however, are for perpendicular incidence only. The target thickness for each incident electron energy and element corresponded to the electron range, or slightly greater, at that energy in a layer of the particular element as computed by Berger and Seltzer<sup>3</sup> in the continuous slowing down approximation. The target thicknesses are given in units of  $\text{g}/\text{cm}^2$  in the figures showing the spectra at different emission angles. The total transmission spectra were derived from the angular data and therefore relate to the same targets as the spectra differential in angle.

Comparisons of bremsstrahlung intensity spectra, differential in angle and photon energy, generated by the electron diffusion program ETRAN 15 of Berger and Seltzer to experimental spectra are shown for Al, Fe, and Au at incident electron energies of 1.0 and 2.8 MeV at several emission angles. Comparisons of total transmission spectra are given at 1.0 MeV for Be, Al, Fe, Sn, and Au and at 2.8 for Al, Fe and Au. The program was run with parameters selected so as to reproduce the experimental conditions. Target thicknesses were input in  $\text{g}/\text{cm}^2$ . The cross-section values selected for use in the calculations were those based on the Bethe-Heitler theory and the experiments of Aiginger and Rester and Dance<sup>4</sup>. The experimental values were used by Berger and Seltzer to re-normalize the values from the Bethe-Heitler theory so that the total radiative yield agrees with the experimental yield. With this method of correction the angular distributions and the spectral

shapes from the Bethe-Heitler theory are not affected. In the energy range spanned by the present comparison, the approximate cross-section values obtained in this way are significantly different from the measured values for Sn and Au at 1.0 MeV. The expected range of electron energy and atomic number for which the approximation may be poor is for electron energies below 2.0 MeV and atomic numbers above 40. The choice of other parameters used in the calculations which are considered important is discussed in the Appendix.

Two sets of calculations were made to generate the computed spectra. The first calculations consisted of runs in which the electrons were followed until their energies fell below about 5% of the incident energy. For a typical run 10,000 electron histories were followed in this manner. It was found, however, that for some backward angles, the statistical accuracy of the computed spectra above 75% of the end point energy was poor, preventing a valid comparison to experiment. To increase the accuracy, additional calculations were made, this time for 40,000 electron histories, but with a cutoff electron energy of 60% of the end point. Each of the computed spectra shown in the comparisons is a composite in the sense that the additional data above 60% of the end point energy have been averaged in. An example of the effect of this procedure is seen in Fig. 1 for the 150-deg spectrum. At about the midpoint of the spectrum, fluctuations begin to occur, while above this point the spectrum again becomes smooth because of the additional histories followed in this region.

The comparisons for Al, Fe, and Au at 1.0 MeV incident electron energy are shown in Figs. 1-3. The values plotted are intensities derived by multiplying the number of photons per energy interval per unit solid angle by the energy of the midpoint of a particular interval as a function of photon energy. The calculated spectra shown here, and at 2.8 MeV, are averaged over 10-deg angular intervals with the midpoints of the intervals equaling the experimental angles as designated in the figures. The experimental values are plotted as points, and the

calculations are plotted as histograms. Agreement between the two sets of spectra is seen for Al and Fe in Figs. 1-2. Comparisons are shown for both of these elements at 15, 45, 75, and 150 deg. For the case of Au the comparison at 1.0 MeV, Fig. 3, revealed an average disagreement between the experimental and calculated values of about 30% above 40% of the end point energy, with the calculated values falling below the experimental values at all three angles shown. A difference of this magnitude exceeds the limits of experimental error. Below 30% of the end point energy the two sets of spectra are essentially in agreement, with the calculations correctly predicting the strong attenuation in the target observed experimentally at 60 deg.

Similar comparisons for Al, Fe, and Au are shown at 2.8 MeV incident electron energy in Figs. 4-6. At this energy good agreement is seen for all three elements. For the Al and Fe targets comparisons are shown at three forward angles and at one backward angle. For the Au target only three forward angles were considered for comparison.

Comparisons of the total transmission spectra reveal substantially the same trends as were observed for the comparisons at various angles. At 1.0 MeV, where significant differences occurred between the calculated and experimental spectra at the various angles, comparisons of the total transmission spectra are shown for Be, Al, Fe, Sn, and Au to allow a more detailed look at the trend with atomic number of the target material. It is seen in Figs. 7-8 that the discrepancy between the calculations and the experiment systematically increases with atomic number, especially in the region of the spectrum above 30% of the end point energy. At 2.8 MeV, where comparisons at angles for Al, Fe, and Au revealed agreement between the calculations and the experiment, agreement is also observed in the comparisons of the total transmission spectra, although above 2.0 MeV photon energy the experimental spectra are somewhat higher than the calculated spectra.



Comparisons of the angular distributions of bremsstrahlung intensity at 1.0 and 2.8 MeV are shown in Figs. 10-11. The calculated points are shown as triangles. These comparisons as expected reveal agreement at both energies for Al, but a significant discrepancy for Au at 1.0 MeV. Of interest is the shape of the angular distributions predicted by the calculations. At angles slightly greater than 90 deg, the intensity rises rapidly, reaching a maximum at about 100 deg. In Fig. 12 the curves depicting the radiated energy as a function of incident electron energy are shown with both experimental values (circles) and calculated values (triangles) at 1.0 and 2.8 MeV. The curves are least squares fits to the experimental points. The calculations are found to agree with the experimental points within the estimated experimental error. Except for the 1.0 MeV Au point, the agreement is real. At 1.0 MeV for Au the apparent agreement is due to the cancellation of differences in averaging over angle.

The differences observed between the calculated spectra and the experimental spectra result from the lack of complete bremsstrahlung cross-section data in the calculations. The approximate cross sections used in the present case are not good enough in the low energy region for high atomic numbers. In Fig. 13 the total cross sections differential in photon energy for Au taken from DATAPAC for 1.0 MeV are shown, as are the total cross sections derived from the experimental cross-section measurements. Although the two curves cross, the values used in the calculation are a factor of two below the experimental curve near the end point energy of 1.0 MeV. At lower electron energies the differences in the two sets of cross section values are comparable near the end points. The result of these large discrepancies is that the high energy thick target bremsstrahlung yield is significantly under-predicted in the calculations.

## ELECTRON TRANSMISSION OF THICK TARGETS

Measurements of electron penetration of thick targets have been reported<sup>2,5</sup> for both perpendicular and non-perpendicular incidence of the electron beam to the target. For the case of normal incidence measurements were made at 1.0 and 2.5 MeV on Al and Au targets, for target thicknesses of 0.2 the range and greater, as given by Berger and Seltzer.<sup>3</sup> The measurements resulted in a set of energy spectra of transmitted electrons at angles with respect to the incident beam between 0 and 90 deg on the transmission side of the target.

For targets of thicknesses of 0.4 the range and greater, electron diffusion is established in the target material before penetration occurs. Because of the diffusion distribution electrons penetrating the target are found to have axial symmetry with respect to the normal to the target, regardless of the angle of incidence. To measure the energy distribution of the transmitted electrons for an omni-directional electron flux, which includes all angles of incidence, it is necessary to measure only a limited number of spectra for different angles of incidence and to integrate over incident angle and emission angle. This procedure was followed for two Al targets, a Sn target, and an Au target at 1.0 MeV incident electron energy.

Comparisons of the experimental spectra at 7.5, 47.5, and 77.5 deg for perpendicular incidence to corresponding spectra from ETRAN 15 are shown in Figs. 14-19 at an incident energy of 1.0 MeV for Al targets of thicknesses corresponding to about 0.2 and 0.4 the range. The region of the distribution in which most of the yield occurs has been plotted on an expanded energy scale to allow more accurate comparison of the two spectra. At 7.5 and 47.5 deg the two sets of spectra are very similar in shape, although the experimental yield at 7.5 deg exceeds the calculated yield by about 15%. At 77.5 deg the statistical fluctuations in the calculated spectrum allow only a qualitative comparison of the two spectra. Similar comparisons for an Au target at 1.0 MeV are shown in Figs. 20-22; however, even for the

thickness corresponding to 0.2 the range, the statistical uncertainties in the calculated Au spectra are quite large. At 7.5 deg the solid angle increment is relatively small and the resulting statistical fluctuations are apparent in the calculations. At 37.5 and 57.5 deg a reasonably good comparison can be made. The experimental values are approximately 20% above the calculated values.

Comparisons of the total transmission spectra for three thicknesses of Al and two thicknesses of Au for an incident electron energy of 1.0 MeV are shown in Figs. 23-27. In Fig. 23 the spectra from an earlier electron diffusion program of Berger and Seltzer is indicated by dashed lines.<sup>5,6</sup> The refinements which have been incorporated into ETRAN 15 result in introducing additional straggling in the distributions. The older calculation was for a target of 0.11 g/cm<sup>2</sup> whereas the calculation with ETRAN 15 was carried for a thickness of 0.10 g/cm<sup>2</sup> as indicated in the figure.

Comparisons of the angular distributions for the measurements at 1.0 MeV are shown in Figs. 28-29.

At 2.5 MeV incident energy somewhat better agreement is observed between the calculated and experimental yields. In Figs. 30-34 comparisons are shown at several angles for the two Al targets for which measurements were made at this energy. Since the measurements were not made at mid-point angles of the angular bins used in the calculation, two calculated spectra are plotted in each figure except in Fig. 30 for 0 deg. The angle of the experimental spectrum corresponds to the boundary of the two angular bins, with one bin averaging over a 5-deg increment at smaller angle than the experimental angle and one bin over a 5-deg increment at larger angle.

The total transmission spectra for the Al and Au targets in Figs. 35-38 indicate agreement between the experiment and the calculations at 2.5 MeV in spectral shapes and total yields within the



experimental error. A total of 20,000 electron histories were followed to obtain the calculated spectrum shown in Fig. 38 where the transmitted fraction was only 8%. Good agreement was also observed in the comparisons of the angular distributions shown in Fig. 39.

Comparisons of calculated and experimental spectra for the case of non-perpendicular incidence are shown in Figs. 40-42. A total of 100,000 electron histories were followed in the calculations. In Fig. 40 the comparisons for two Al targets are shown. The experimental points are indicated by open circles and the calculated by solid points. The spectra, and those for Sn and Au, represent total transmission spectra for an incident electron flux distributed in intensity as the cosine of the angle of incidence. The ordinate of the plot gives the number of transmitted electrons per incident electron averaged over the cosine distribution. The differences between the calculated and experimental spectra for the Al and Sn targets seen in the figures are in the direction expected in light of the approximations made in constructing the experimental spectra. The somewhat larger difference in the yields seen in the comparison for the Au target, however, exceeds that expected from the approximation alone.

## BREMSSTRAHLUNG CROSS SECTIONS

Experimental bremsstrahlung cross-section values were reported for Al, Cu, Sn, and Au at incident electron energies of 0.2, 1.0, 1.7 and 2.5 MeV.<sup>1,7</sup> Measurements at 0.05 MeV were reported for Al and Au.<sup>2</sup>

In the electron energy region from low energy to 3.0 MeV, no theoretical cross-section values are available, except the values calculated by the Born approximation. These values are not generally accurate for all elements in this region. Recently Brysk, Zerby, and Penny<sup>8</sup> reported bremsstrahlung cross sections for Au in the electron energy range from 0.180 to 0.5 MeV. Comparisons of the newly computed values to experimental values of Aiginger<sup>9</sup> at 0.180 and 0.380 MeV clearly indicated a discrepancy between experiment and theory at small angles and low photon energies. At 0.5 MeV the computed values were substantially below experimental value at all angles and photon energies.

Since the publication of the paper of Brysk, Zerby, and Penny, modifications to their program have been made which increased the accuracy of the computations. The modifications allowed values for Al to be computed in the low electron energy region, whereas previously oscillations were discernible in the calculated spectra for low-Z elements. The range of electron energy for which accurate calculations can be made was extended to both higher and lower energies.

Comparisons of the theoretical cross-section values from the Brysk-Zerby-Penny formulas to experimental values previously reported are shown at 0.05 and 0.2 MeV for Al and Au targets in Figs. 43-48. It was not possible to obtain accurate theoretical values for an incident electron energy of 1.0 MeV, the next higher energy at which measurements were made.

Agreement between the theory and experiment within the limits of experimental error is seen for Al in Fig. 43 at 0.05 MeV, except at a photon energy of 10 keV. At 10 keV only the point at 120 deg agrees with the theory. At 10 keV photon energy for Au in Fig 44, three of the five experimental points are right on the theoretical curve. The point at 20 deg is about 12% high and the point at 10 deg is 20% high.

At an incident electron energy of 0.20 MeV comparisons for Al at photon energies of 46, 76, 106, 166, and 196 keV are shown in Figs. 45-46. Good agreement is observed at all photon energies except for the points at 10 deg at photon energies of 76 and 106 keV, where the experimental points are well above the theory. The trend of the experimental values indicates a maximum at about 10 deg for these photon energies, while the computed values reach maximum values at about 20 deg. In Fig. 47 for Au at a photon energy of 80 keV, or 40% of the end-point energy, a similar trend is observed with the calculated values peaking at larger photon angle. Also shown in the figure are the Born-approximation values, plotted as dashed line curves. At small angles the shape of the Born-approximation curve is similar to the experimental angular distribution, although the magnitudes of the experimental values, except for the 10- and 20-deg points, are in agreement with the newly computed values from the relativistic self-consistent field model. At 120 and 160 keV the agreement between experiment and the values from the modified programs of Brysk, Zerby, and Penny is good except at 10 deg for a photon energy of 120 keV, where the experiment is 20% high. The Born-approximation values are low at the higher photon energies.

A plot of the spectrum at 120 deg for a bombarding energy of 0.05 MeV and an Au target is shown in Fig. 48. The theoretical points are shown at photon energies of 10, 20, 30 and 40 keV.



## APPENDIX

A documentation of the programs used to compute the spectra shown in the present report as comparisons to experiment has been published by Berger and Seltzer.<sup>4,10</sup> Reasonably complete descriptions of the programs are provided, including definitions of the input parameters and the program options available to the user. Program listings and printouts of short runs are also given. To specify the calculations shown in the present report, some of the options selected are listed in this section.

One of the options available is a choice of electron bremsstrahlung cross-section values. This choice for the energy range presently considered greatly affects the thick-target bremsstrahlung yields, but probably has only a small effect on the transmitted electron yields. DATATAPE 2 was used in both the bremsstrahlung and electron transmission calculations shown in the preceding sections (the electron and bremsstrahlung calculations were carried out in separate runs). The cross sections of DATATAPE 2 consist of values from the Bethe-Heitler theory, modified by a set of correction factors dependent on electron energy obtained from the experiments of Aiginger<sup>9</sup> and of Rester and Dance.<sup>1,7</sup>

Two programs were used in the calculations. One of these, DATAPAC 4, accepts basic data, including the cross sections described above, to produce tabular arrays of information. The second program, ETRAN 15, generates electron and photon histories by random sampling on the basis of the information from DATAPAC 4. To calculate the spectra shown in this report, input parameters values in DATAPAC 4 were selected so that:

- (1) the Mott scattering cross sections were used;
- (2) a screening function from the Moliere theory was used;

- (3) energy loss was logarithmic with successive energies reduced by a constant factor; and
- (4) for Al, Fe, and Sn the number of grid intervals to reduce the energy by a factor of two was 8; for Au, 16.

Choices of input parameter values of ETRAN 15 were made so that:

- (1) energy loss straggling was considered;
- (2) knock-on delta rays were included;
- (3) directions of primary electrons were unchanged after inelastic collisions;
- (4) histories of secondary photons were followed;
- (5) intrinsic bremsstrahlung emission angles were sampled from cross-section tables;
- (6) target thicknesses were read in  $\text{g/cm}^2$ ;
- (7) 10,000 primary electron histories were followed in the thick-target bremsstrahlung calculations; and
- (8) 20,000 primary electron histories were followed in the diffusion spectra.

## REFERENCES

1. W. E. Dance, W. J. Rainwater, and D. H. Rester, "Investigation of Electron Interaction in Matter", NASA CR-1194, Oct. 1968.
2. D. H. Rester, "An Experimental Study of Electron Transmission and Bremsstrahlung Production", NASA CR-1383, Aug. 1969.
3. M. J. Berger and S. M. Seltzer, "Tables of Energy Losses and Ranges of Electrons and Positrons", NASA SP-3012, 1964.
4. M. J. Berger and S. M. Seltzer, "Electron and Photon Transport Programs 1. Introduction and Notes on Program DATAPAC 4", NBS Report 9836, June, 1968.
5. D. H. Rester and W. J. Rainwater, "Investigations of Electron Interactions with Matter Part 2. Electron Scattering in Aluminum", NASA CR-334, Dec. 1965.
6. D. H. Rester and W. J. Rainwater, J. Appl. Phys. 37, 1793 (1966).
7. D. H. Rester and W. E. Dance, Phys. Rev. 161, 85 (1967).
8. H. Brysk, C. D. Zerby, and S. K. Penny, Phys. Rev. 180, 104 (1969).
9. H. Aiginger, Z. Physik 197, 8 (1966).
10. M. J. Berger and S. M. Seltzer, "Electron and Photon Transport Programs 2. Introduction and Notes on Program ETRAN 15", NBS Report 9837, June 1968.



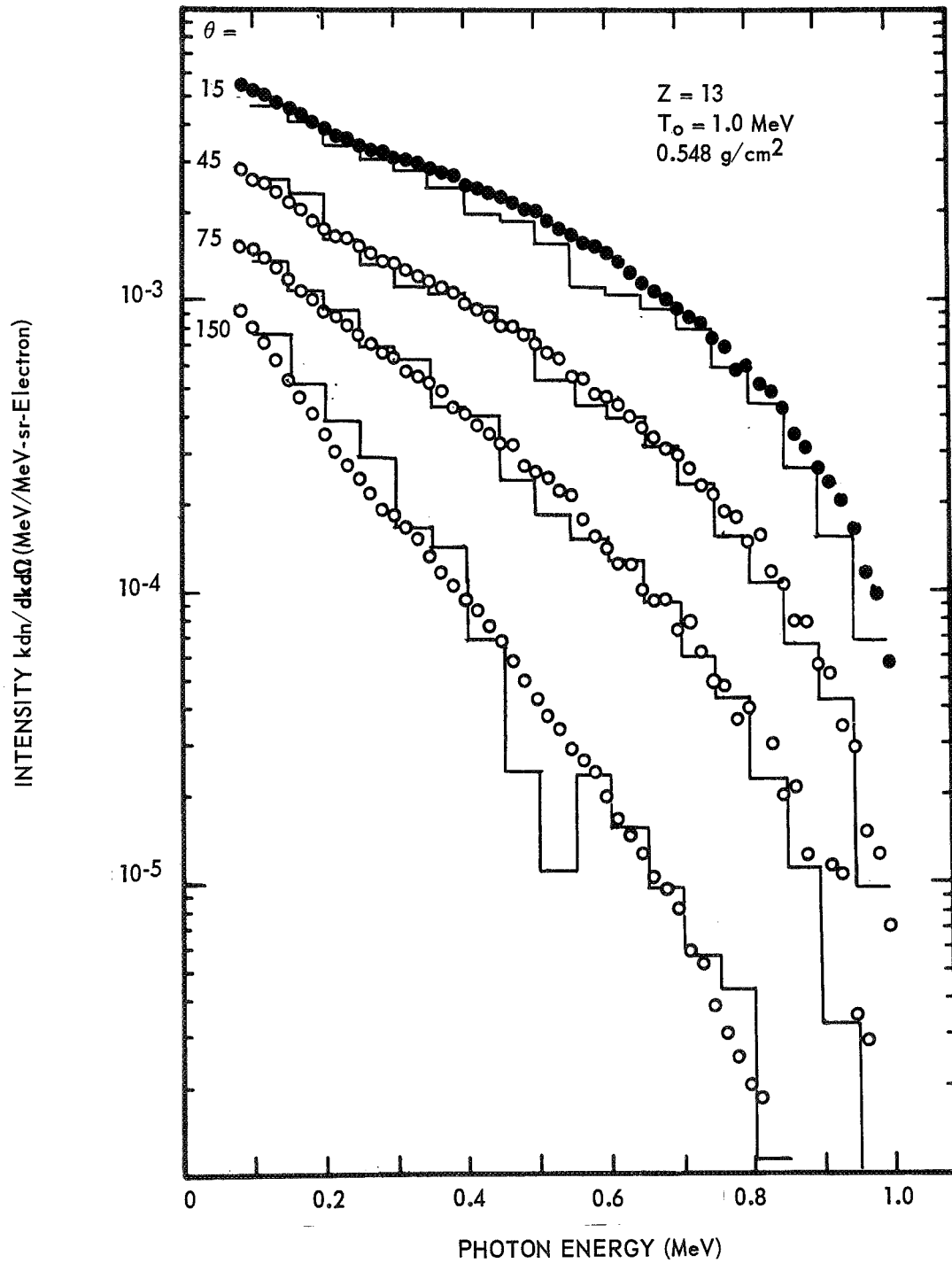


FIGURE 1. COMPARISONS OF EXPERIMENTAL AND CALCULATED BREMSSTRAHLUNG INTENSITY SPECTRA. THE CALCULATED SPECTRA ARE SHOWN AS HISTOGRAMS.

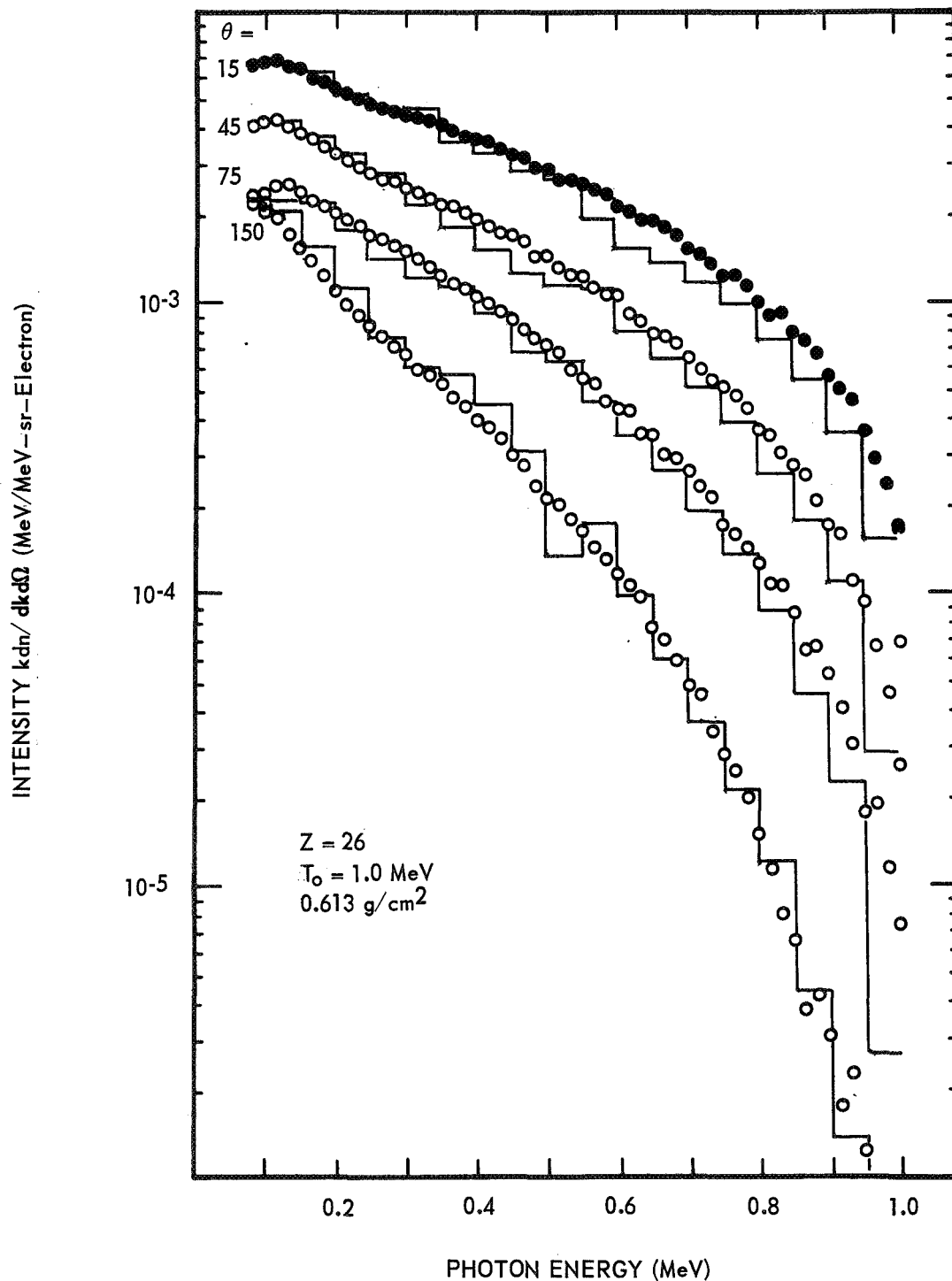


FIGURE 2. COMPARISONS OF EXPERIMENTAL AND CALCULATED BREMSSTRAHLUNG INTENSITY SPECTRA. THE CALCULATED SPECTRA ARE SHOWN AS HISTOGRAMS.

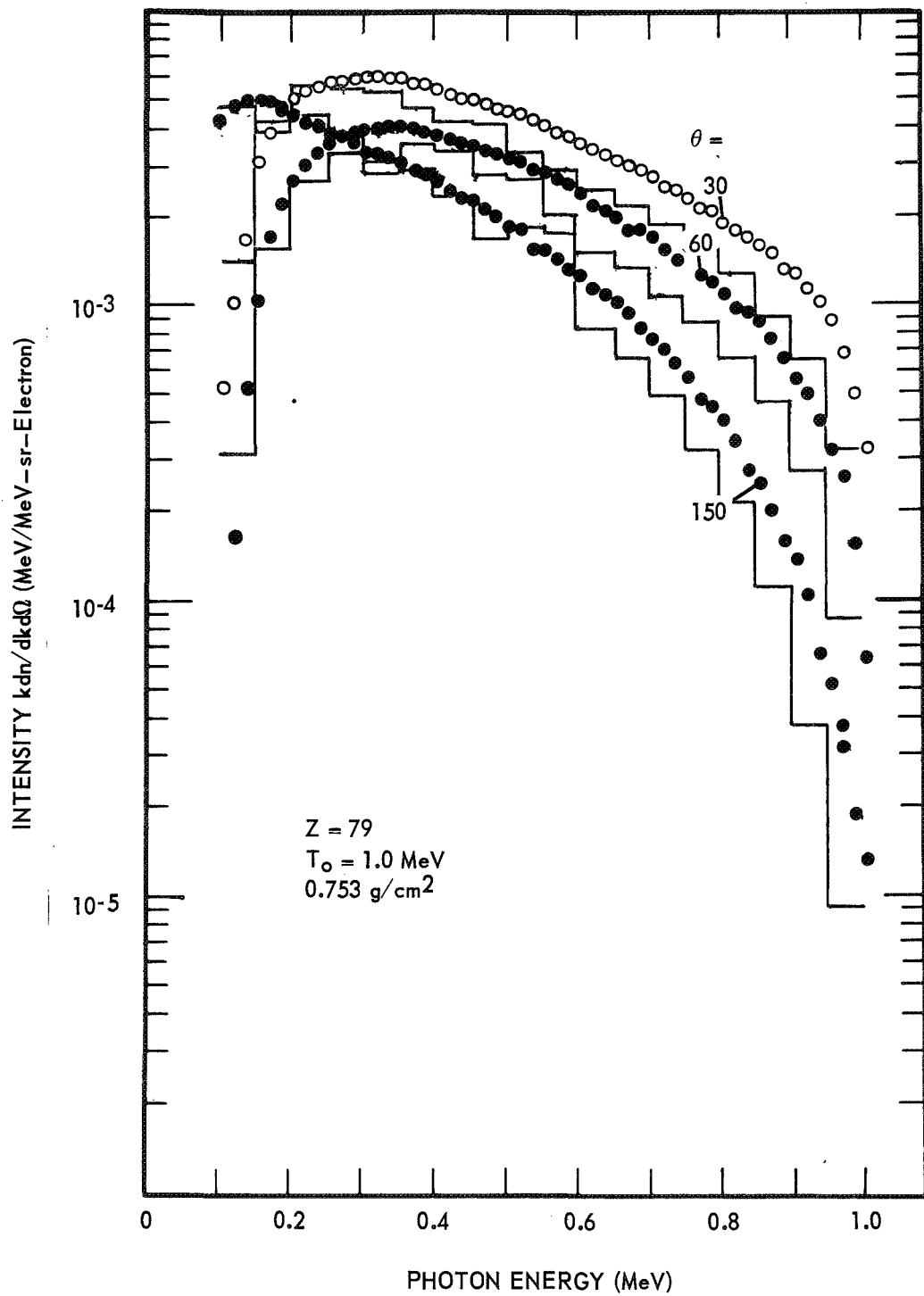


FIGURE 3. COMPARISONS OF EXPERIMENTAL AND CALCULATED BREMSSTRAHLUNG INTENSITY SPECTRA. THE CALCULATED SPECTRA ARE SHOWN AS HISTOGRAMS.

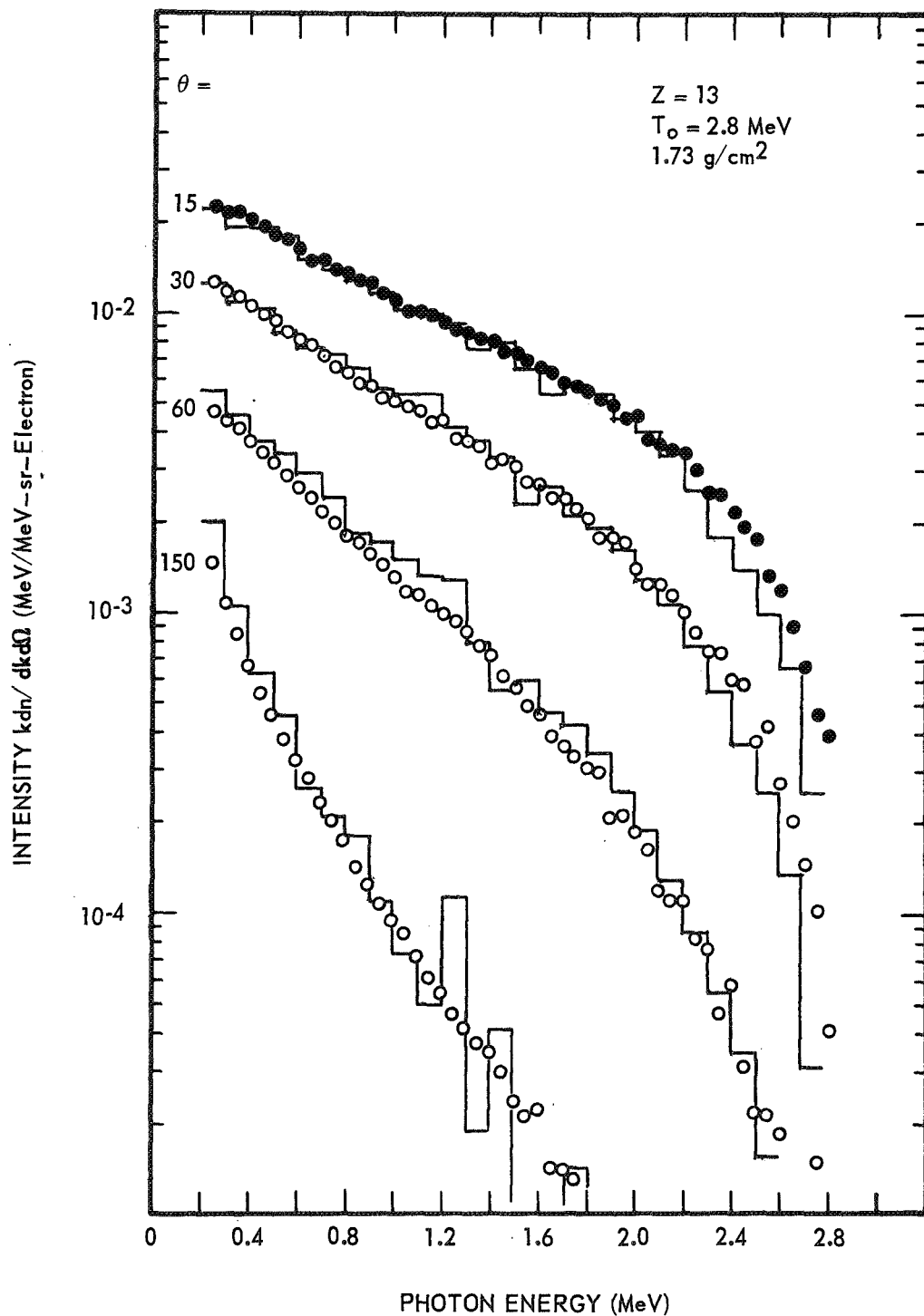


FIGURE 4. COMPARISONS OF EXPERIMENTAL AND CALCULATED BREMSSTRAHLUNG INTENSITY SPECTRA. THE CALCULATED SPECTRA ARE SHOWN AS HISTOGRAMS.

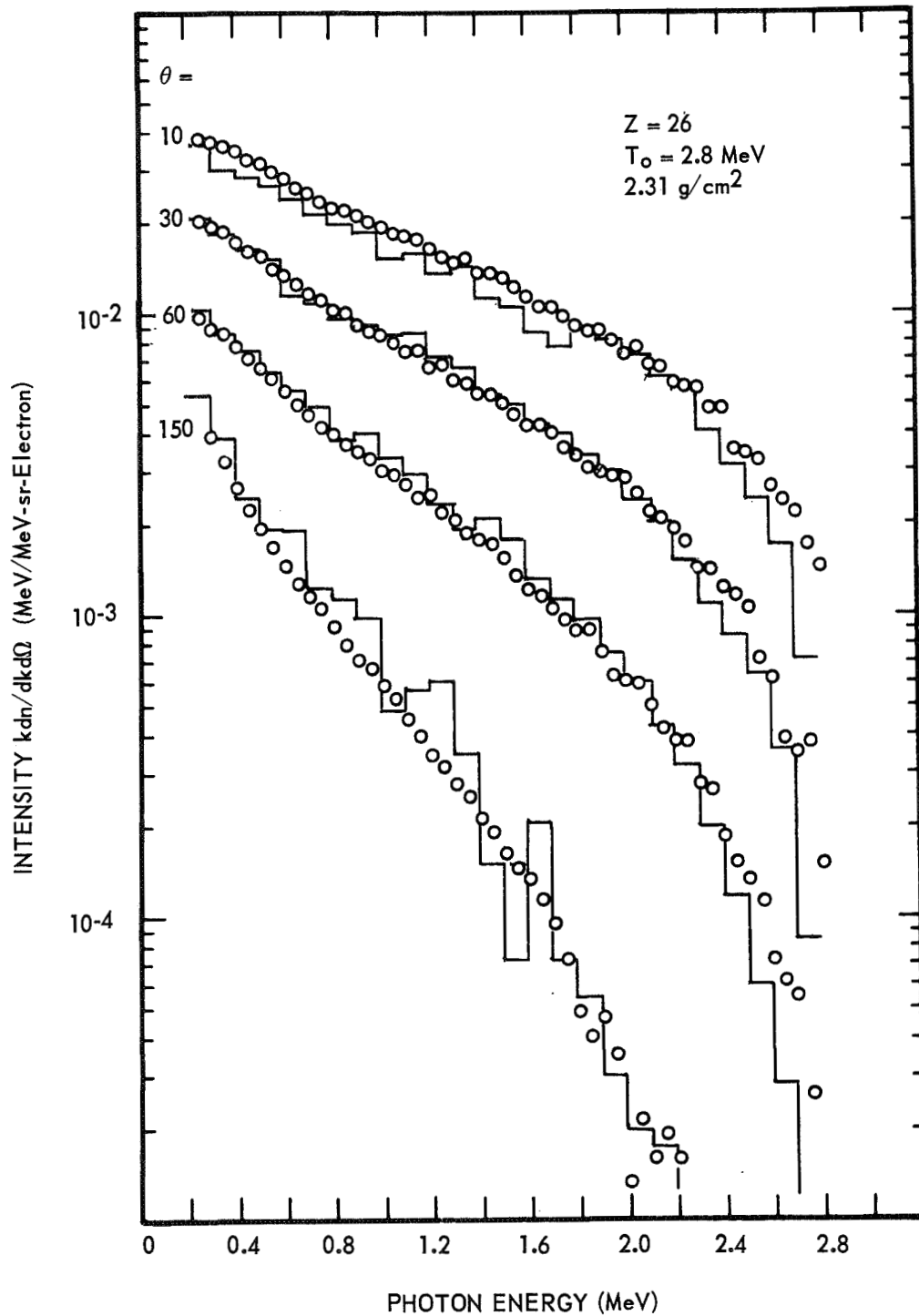


FIGURE 5. COMPARISONS OF EXPERIMENTAL AND CALCULATED BREMSSTRAHLUNG INTENSITY SPECTRA. THE CALCULATED SPECTRA ARE SHOWN AS HISTOGRAMS.

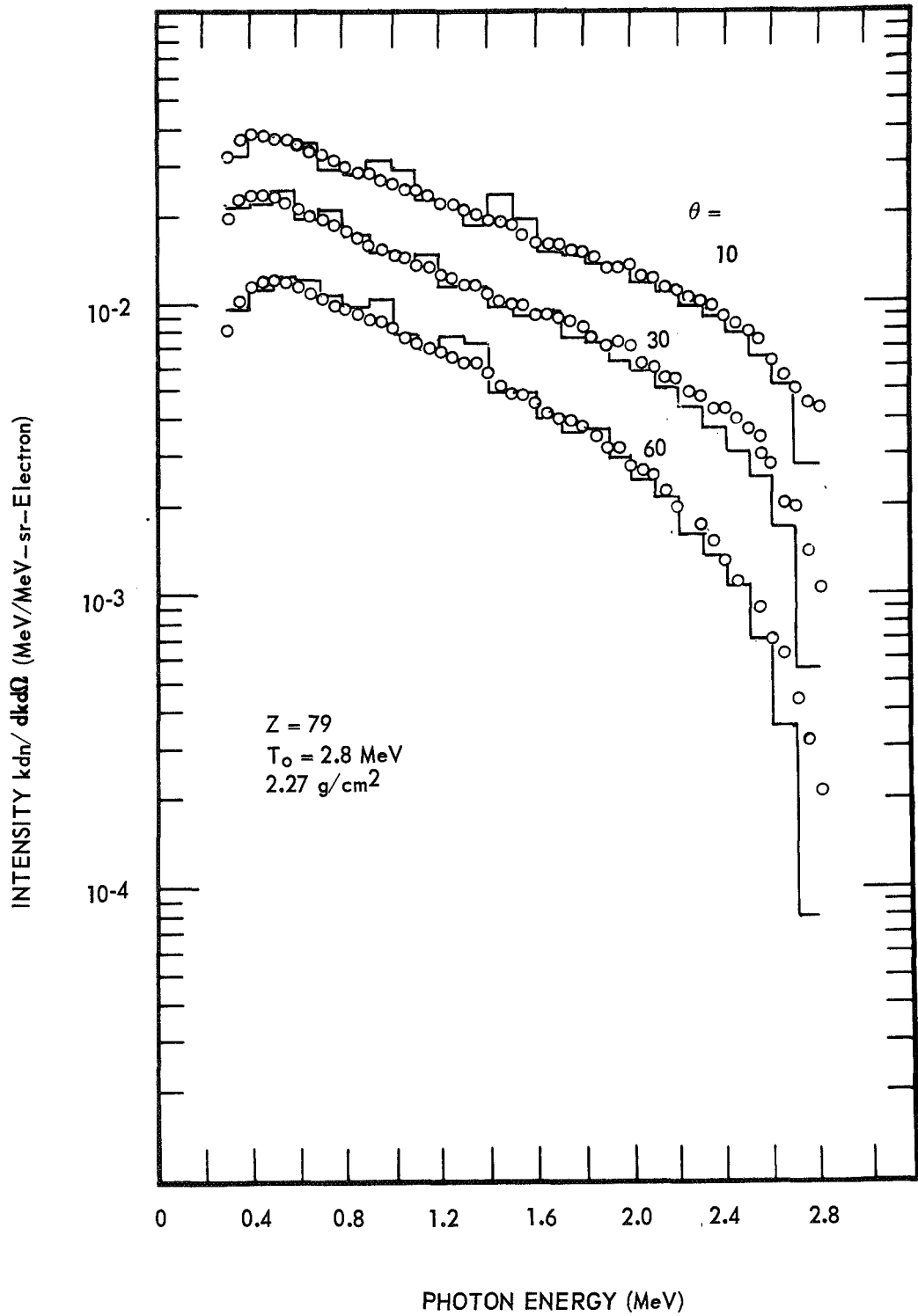


FIGURE 6. COMPARISONS OF EXPERIMENTAL AND CALCULATED BREMSSTRAHLUNG INTENSITY SPECTRA. THE CALCULATED SPECTRA ARE SHOWN AS HISTOGRAMS.



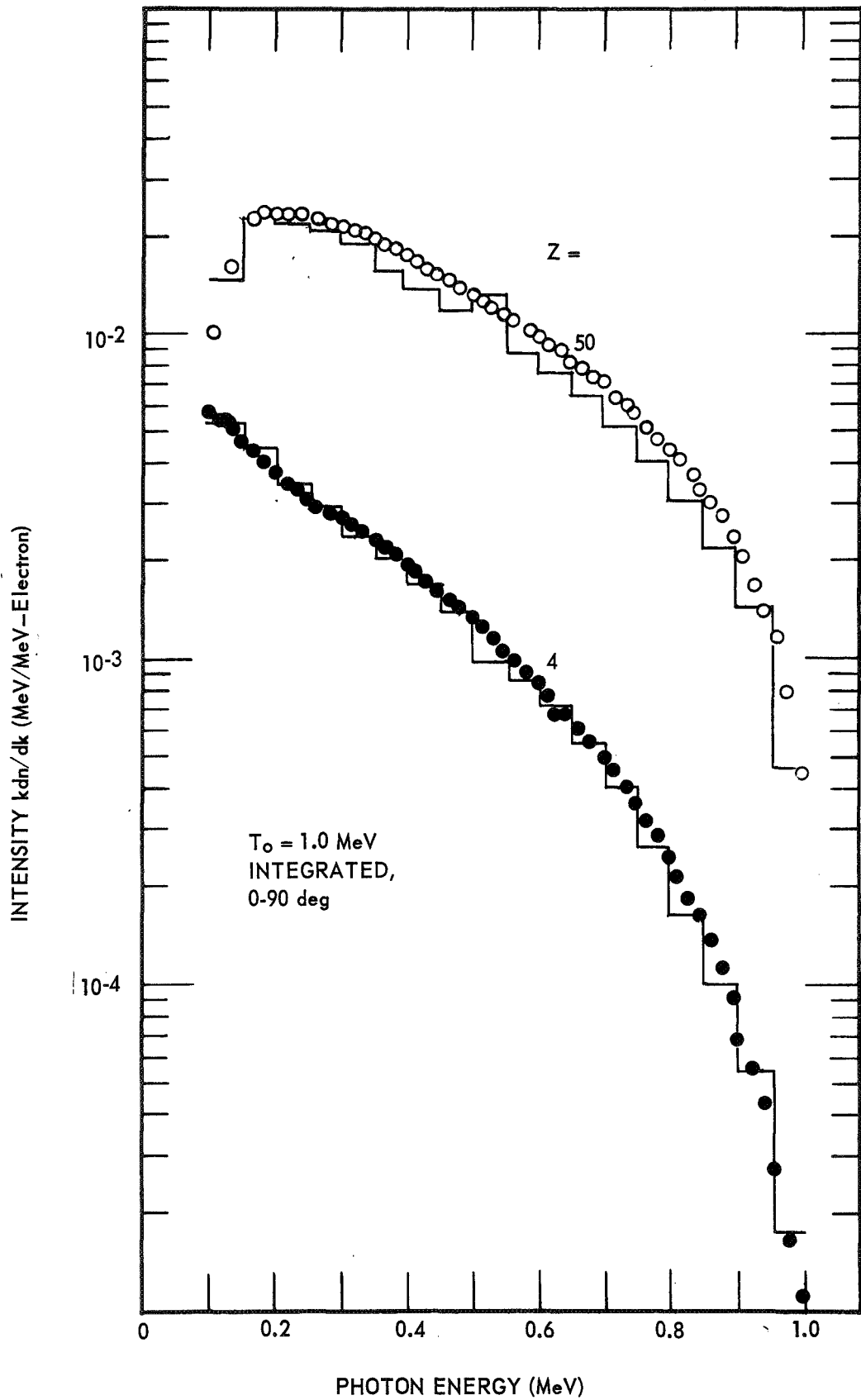


FIGURE 7. COMPARISONS OF EXPERIMENTAL AND CALCULATED TOTAL TRANSMISSION SPECTRA FOR Be AND Sn. THE CALCULATED SPECTRA ARE SHOWN AS HISTOGRAMS.

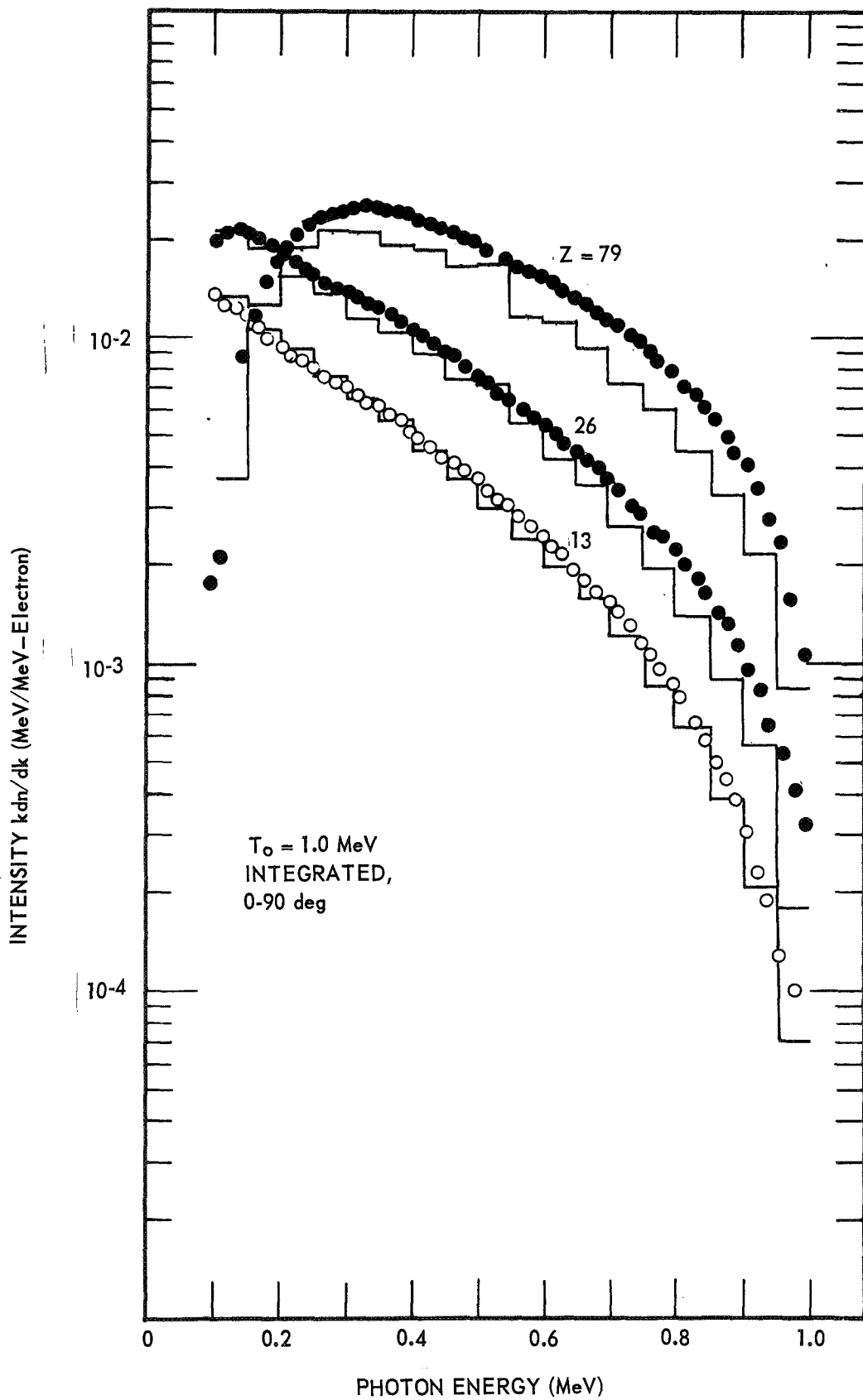


FIGURE 8. COMPARISONS OF EXPERIMENTAL AND CALCULATED TOTAL TRANSMISSION SPECTRA FOR Al, Fe, AND Au. THE CALCULATED SPECTRA ARE SHOWN AS HISTOGRAMS.

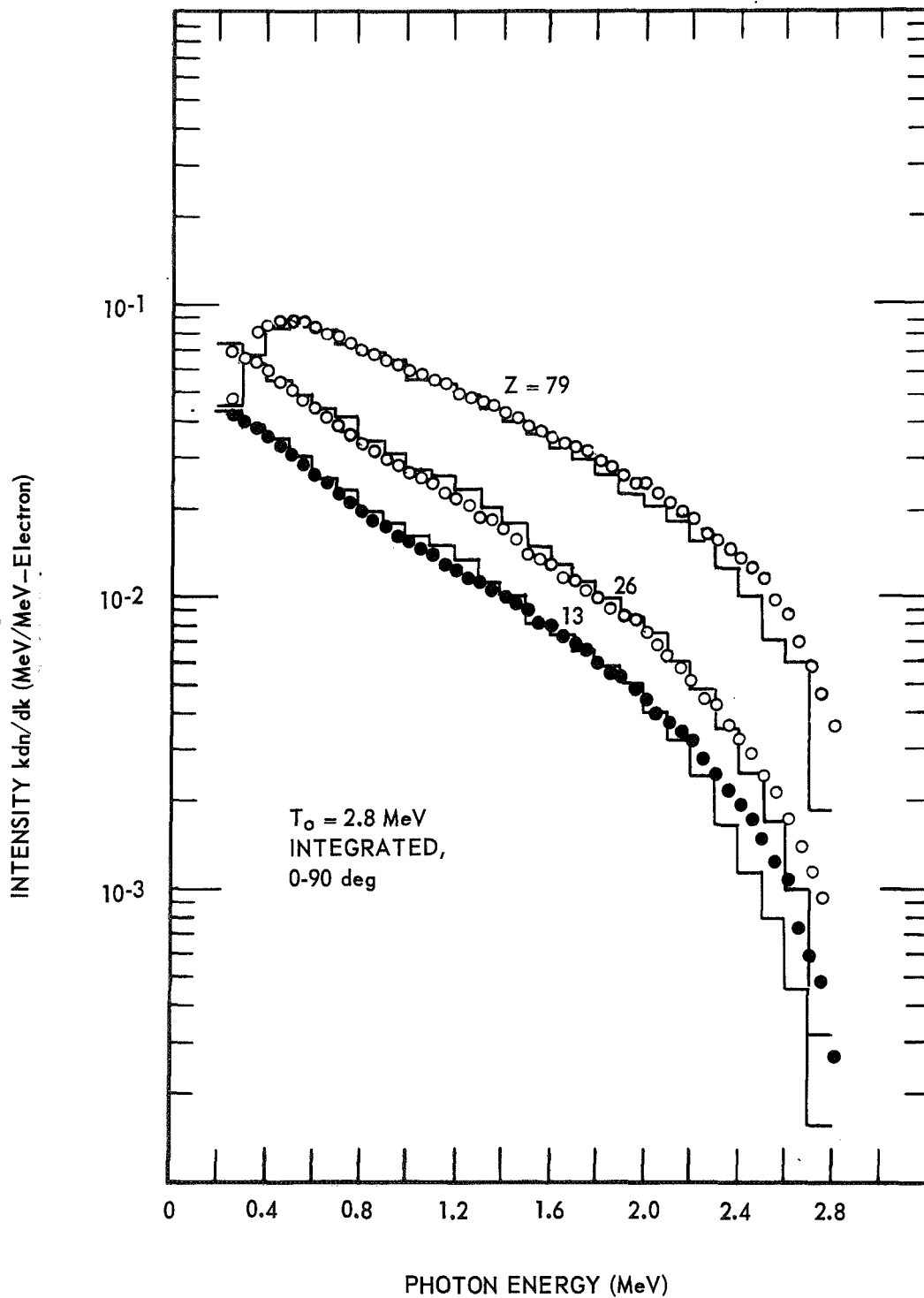


FIGURE 9. COMPARISONS OF EXPERIMENTAL AND CALCULATED TOTAL TRANSMISSION SPECTRA FOR Al, Fe, AND Au. THE CALCULATED SPECTRA ARE SHOWN AS HISTOGRAMS.

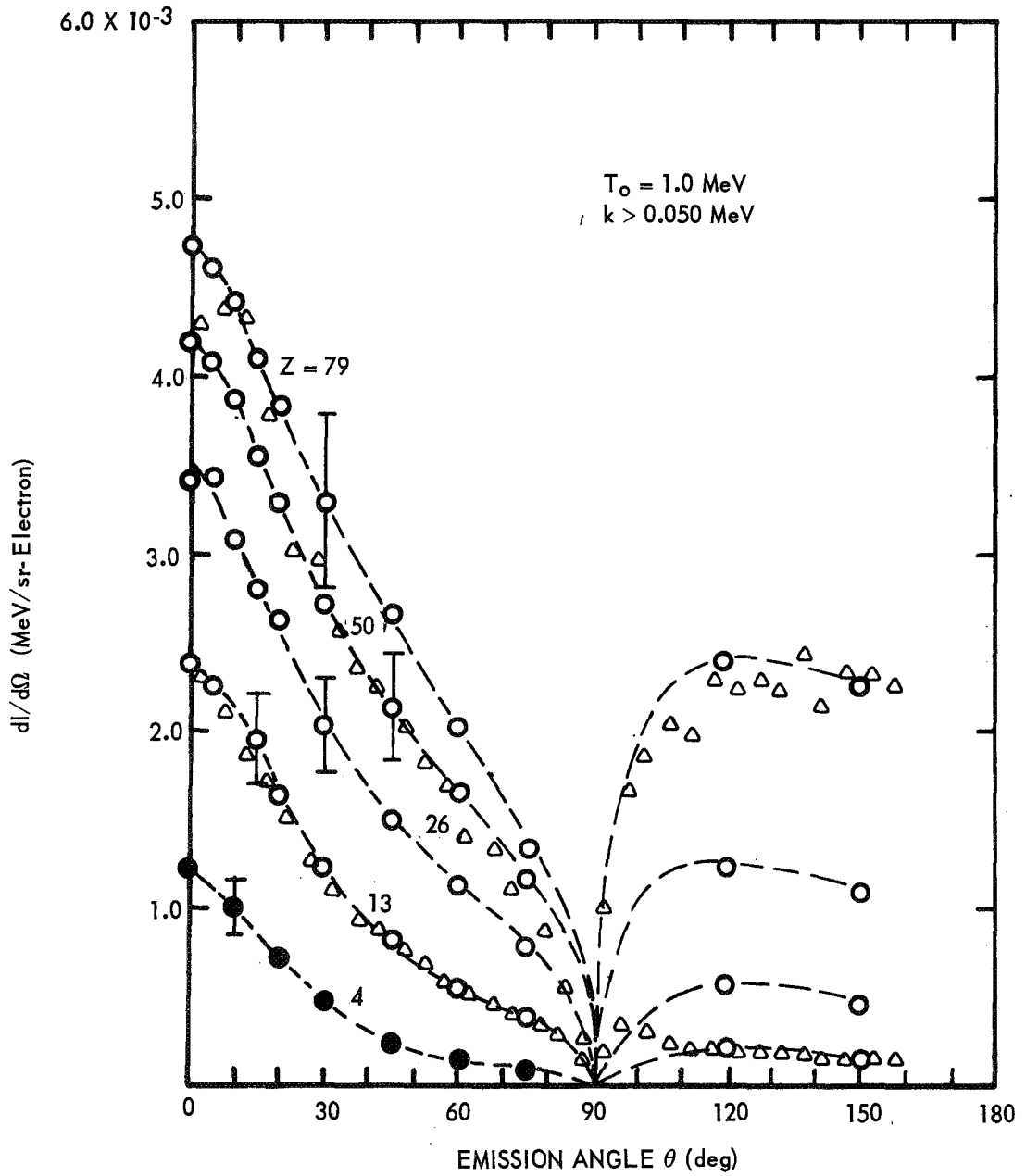


FIGURE 10. ANGULAR DISTRIBUTIONS OF BREMSSTRAHLUNG INTENSITIES, INTEGRATED OVER PHOTON ENERGY,  $k > 0.050$  MeV, FOR 1.0 MeV ELECTRONS ON THICK TARGETS OF Be, Al, Fe, Sn, AND Au. MONTE CARLO CALCULATED VALUES FOR Al AND Au ARE SHOWN AS TRIANGLES.

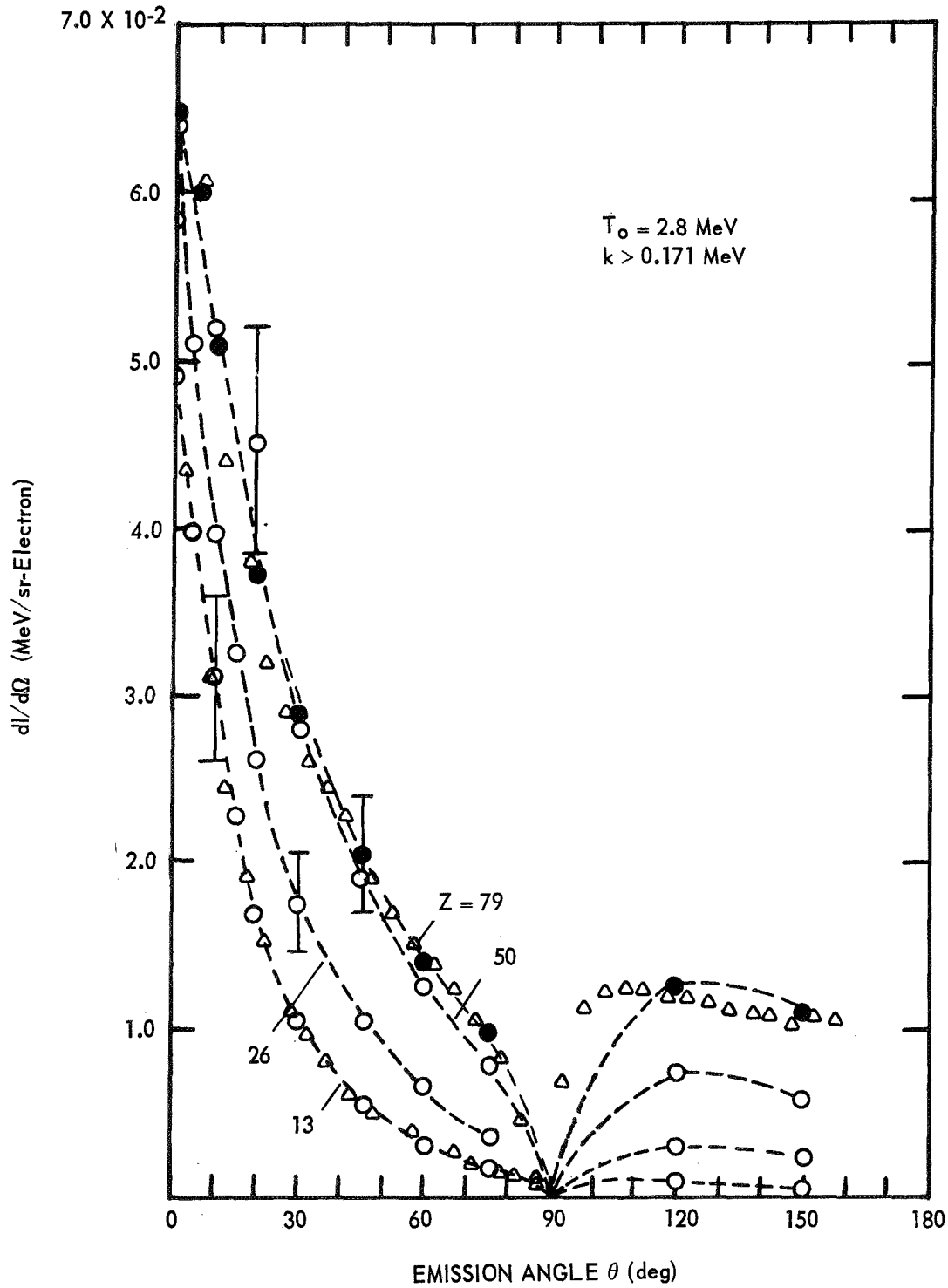


FIGURE 11. ANGULAR DISTRIBUTIONS OF BREMSSTRAHLUNG INTENSITIES, INTEGRATED OVER PHOTON ENERGY,  $k > 0.171 \text{ MeV}$ , FOR 2.8 MeV ELECTRONS ON THICK TARGETS OF Al, Fe, Sn, AND Au. MONTE CARLO CALCULATED VALUES FOR Al AND Au ARE SHOWN AS TRIANGLES.

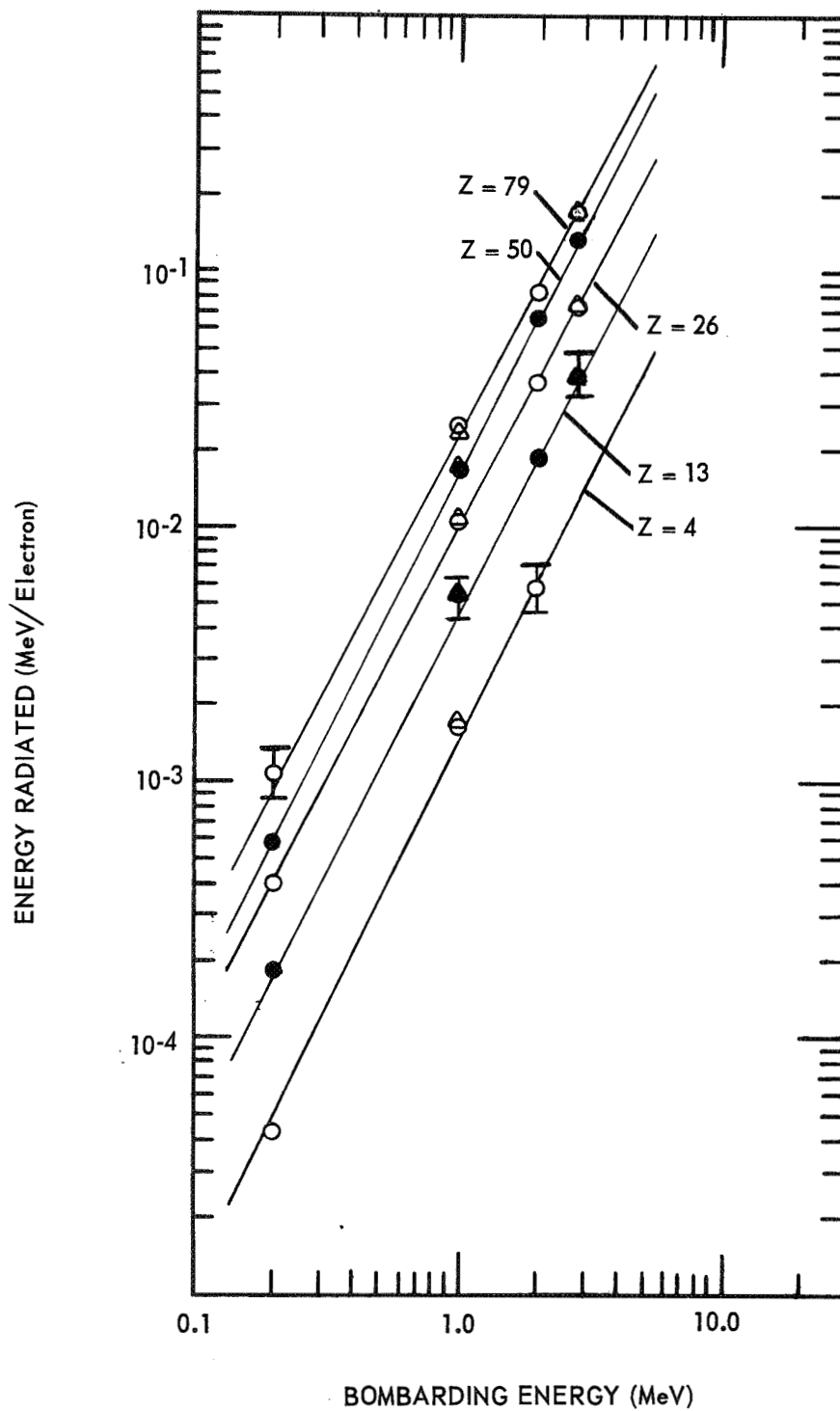


FIGURE 12. COMPARISON OF TOTAL RADIATED ENERGIES. THE LOWER CUT-OFF ENERGIES FOR 0.2, 1.0, 2.0 AND 2.8 MeV ARE 36, 50, 133, AND 171 keV. CALCULATED VALUES ARE SHOWN AS TRIANGLES.



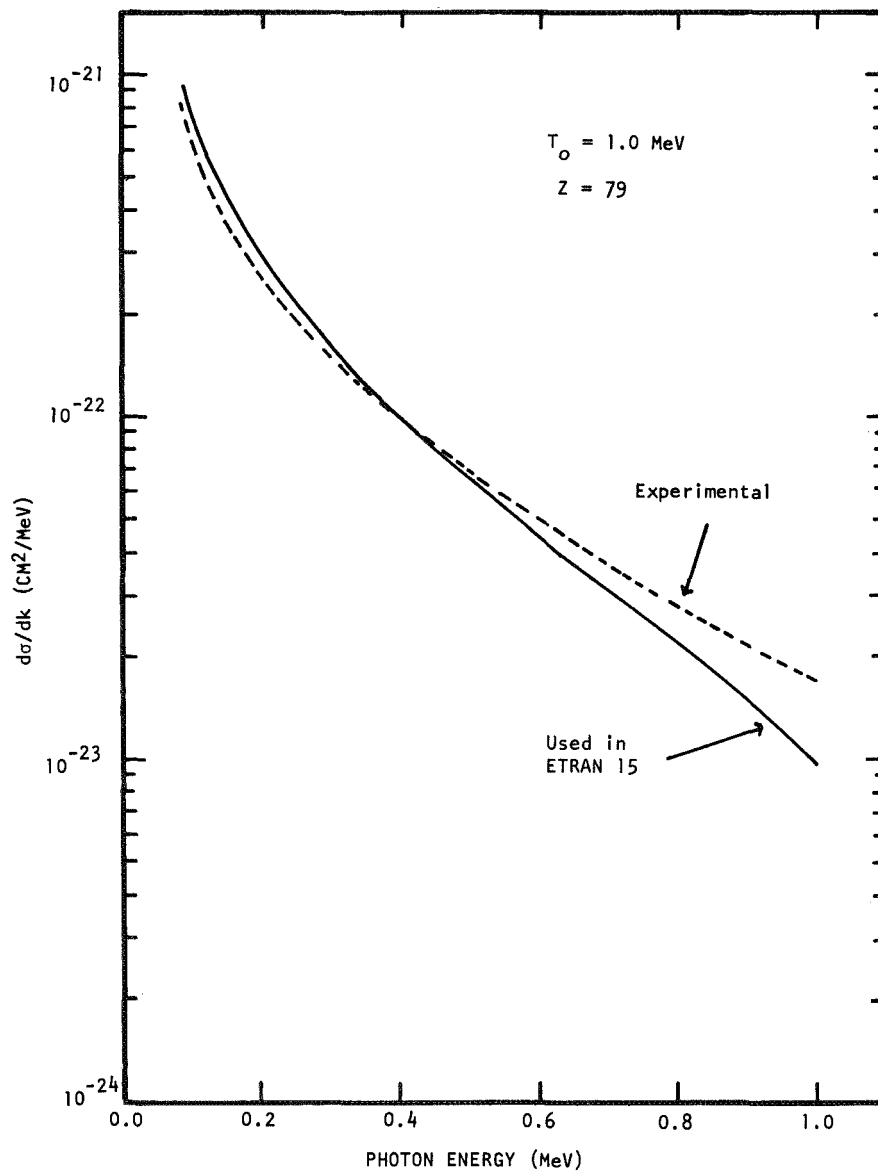


FIGURE 13. TOTAL BREMSSTRAHLUNG CROSS SECTION CURVES. THE DASHED CURVE IS BASED ON EXPERIMENT. THE SOLID LINE CURVE REPRESENTS CROSS SECTIONS USED IN THE CALCULATIONS.

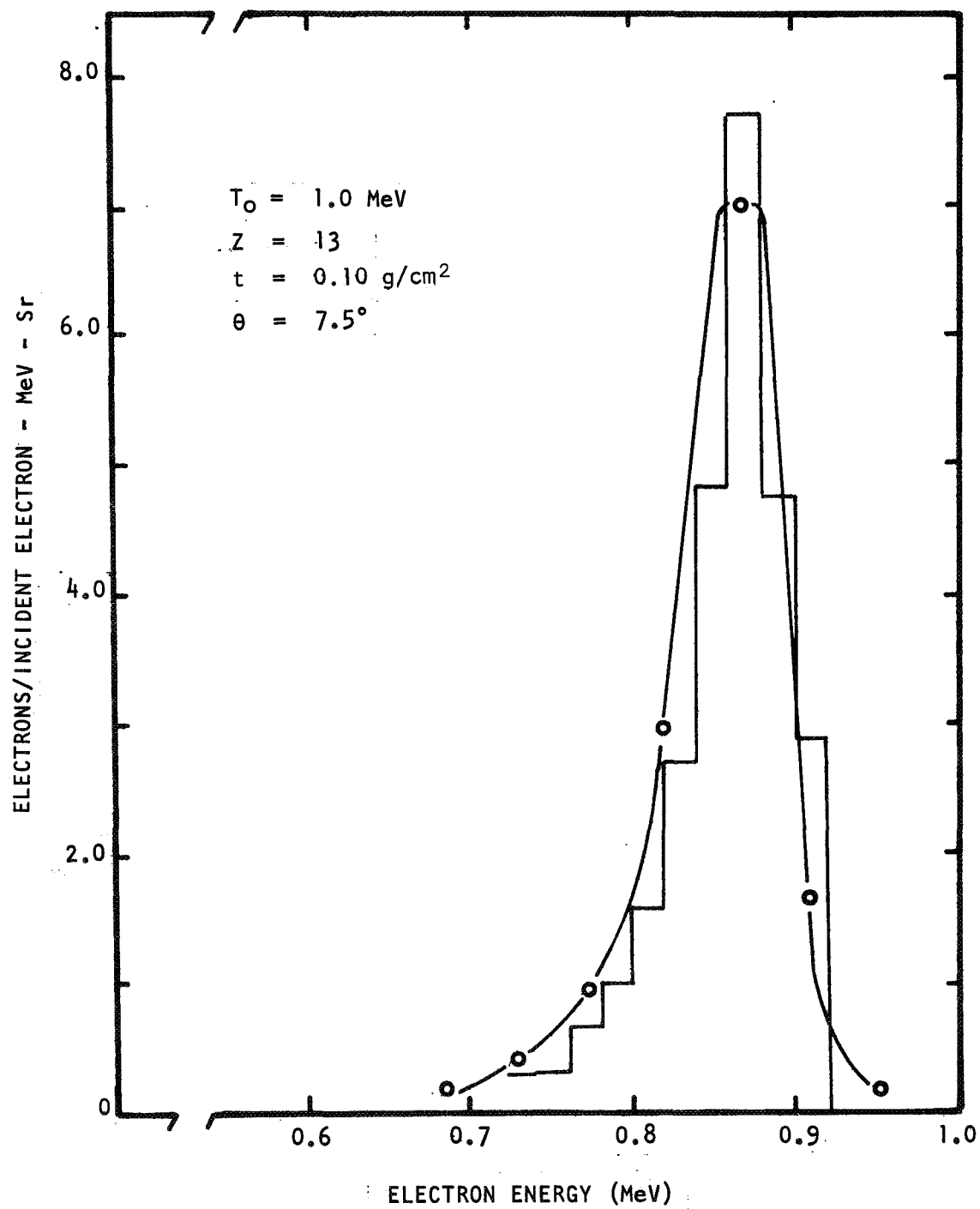


FIGURE 14. COMPARISON OF EXPERIMENTAL AND CALCULATED ELECTRON TRANSMISSION SPECTRA. THE CALCULATED SPECTRUM IS SHOWN IN HISTOGRAM FORM.

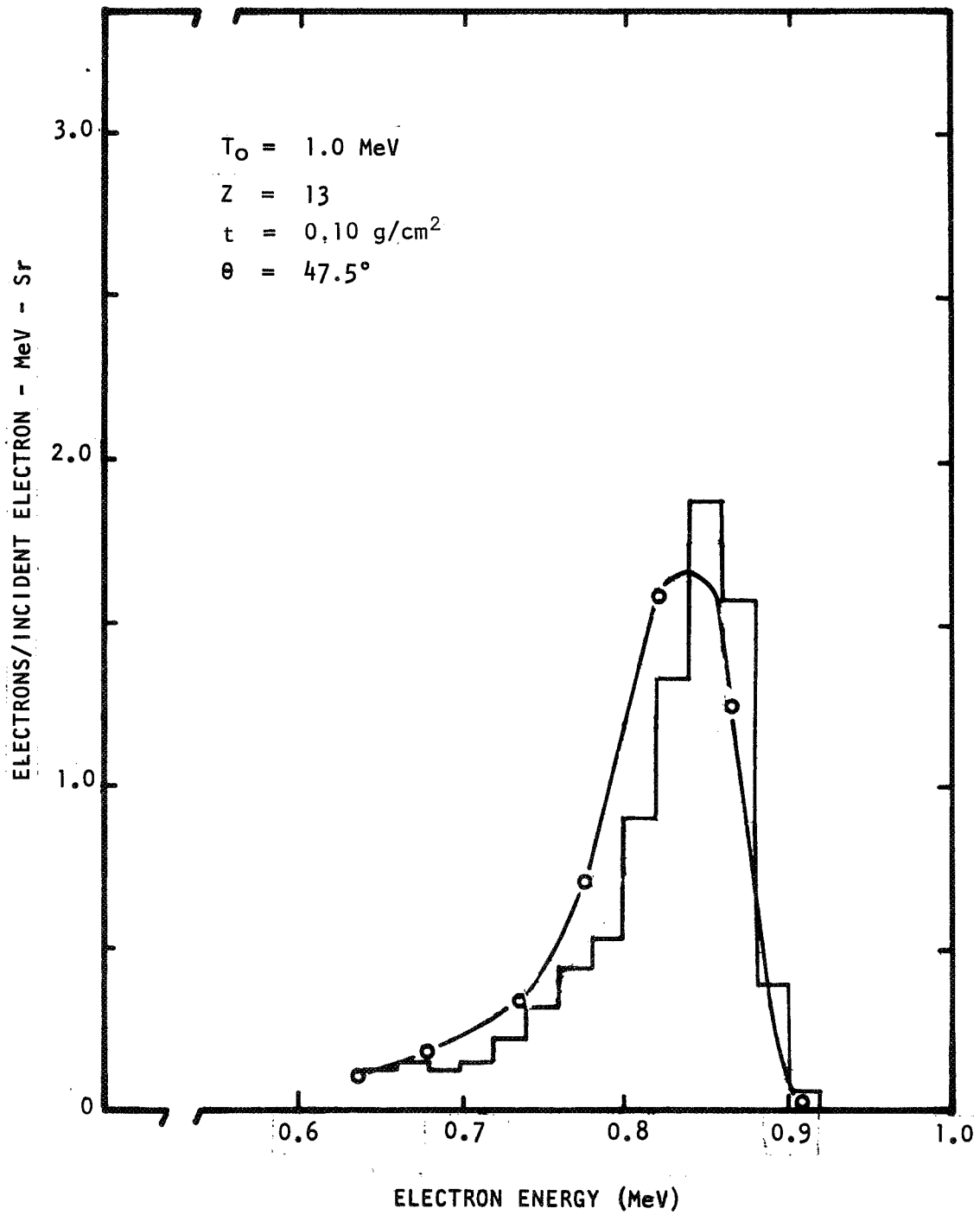


FIGURE 15. COMPARISON OF EXPERIMENTAL AND CALCULATED ELECTRON TRANSMISSION SPECTRA. THE CALCULATED SPECTRUM IS SHOWN IN HISTOGRAM FORM.

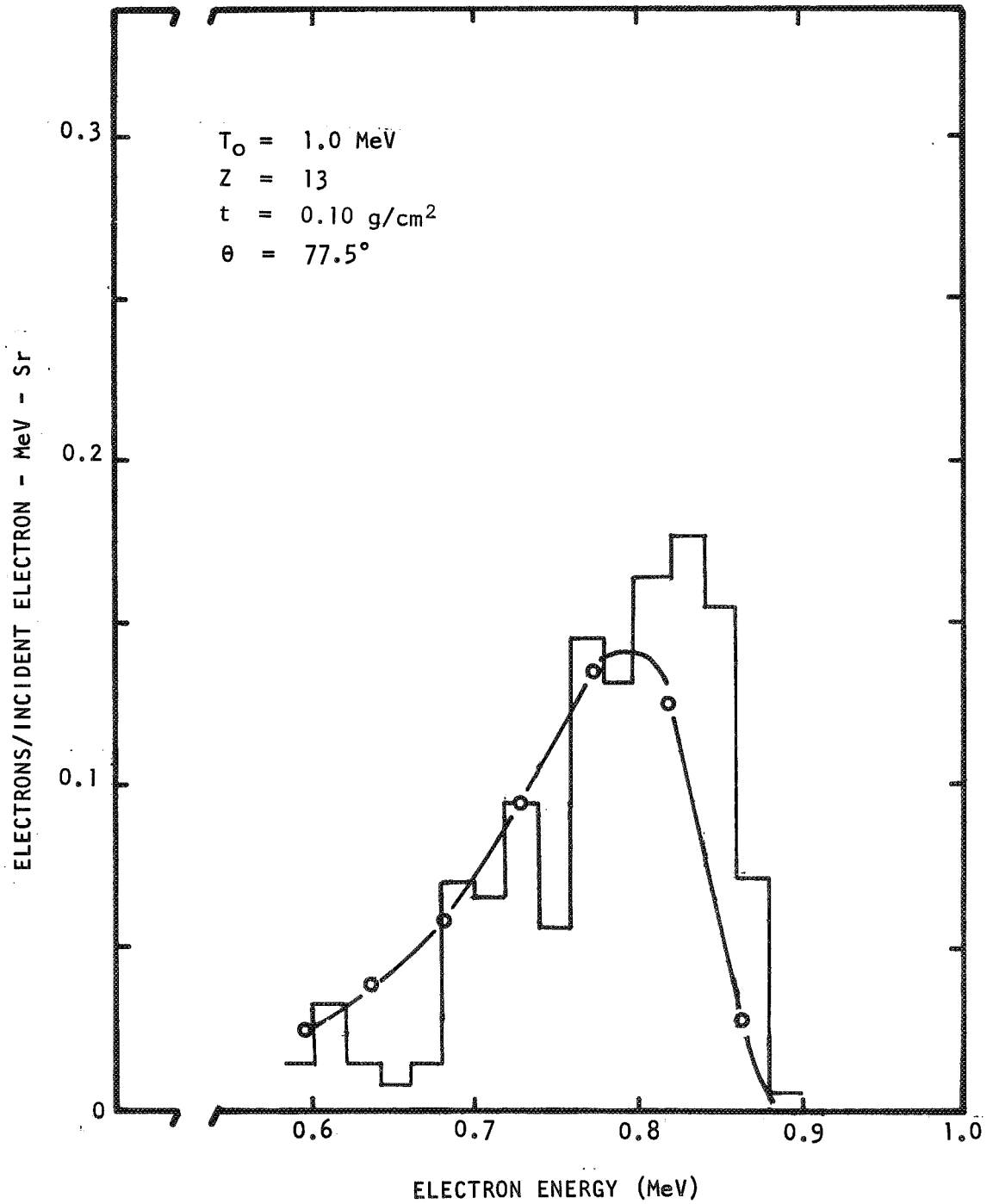


FIGURE 16. COMPARISON OF EXPERIMENTAL AND CALCULATED ELECTRON TRANSMISSION SPECTRA. THE CALCULATED SPECTRUM IS SHOWN IN HISTOGRAM FORM.

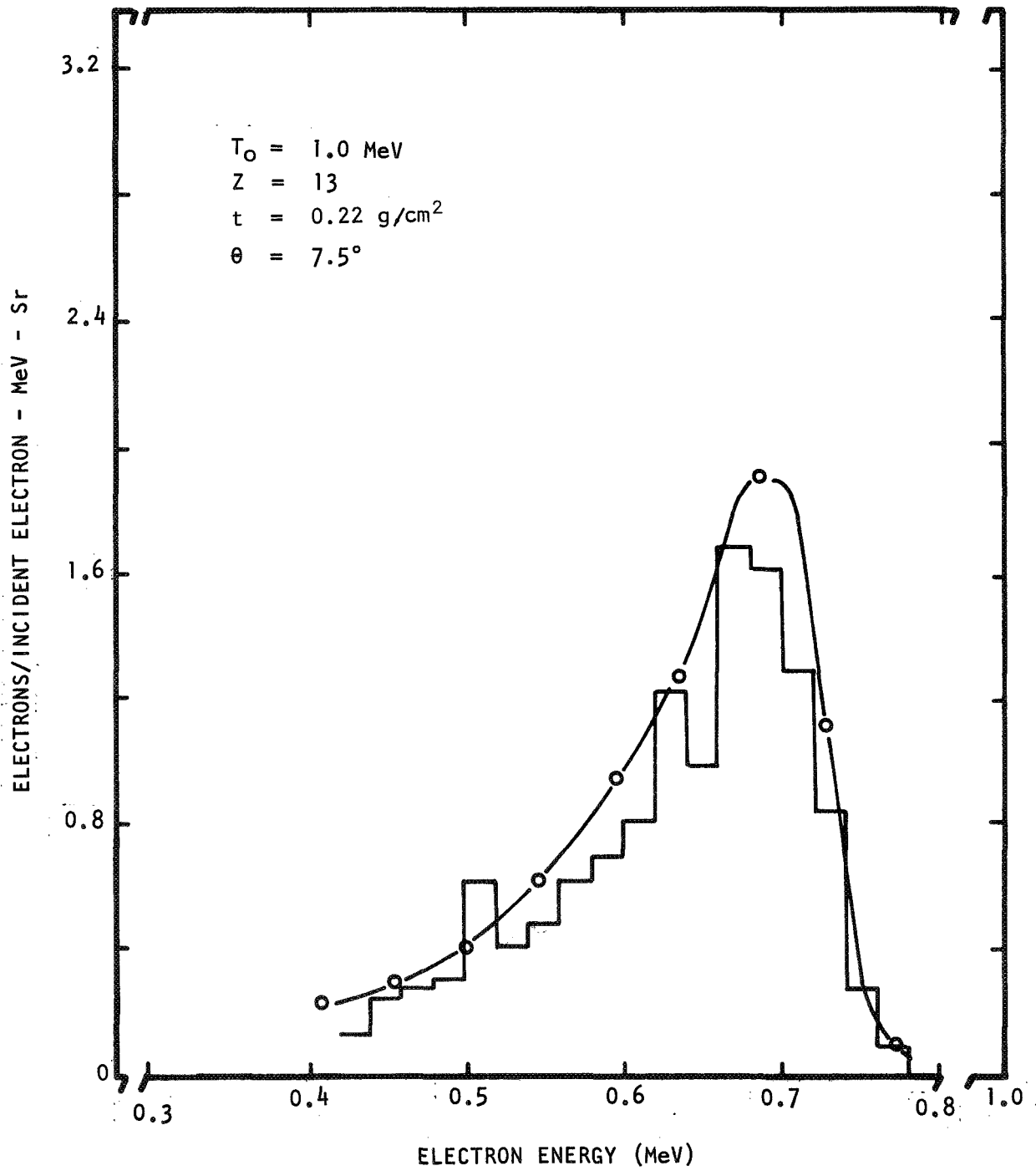


FIGURE 17. COMPARISON OF EXPERIMENTAL AND CALCULATED ELECTRON TRANSMISSION SPECTRA. THE CALCULATED SPECTRUM IS SHOWN IN HISTOGRAM FORM.

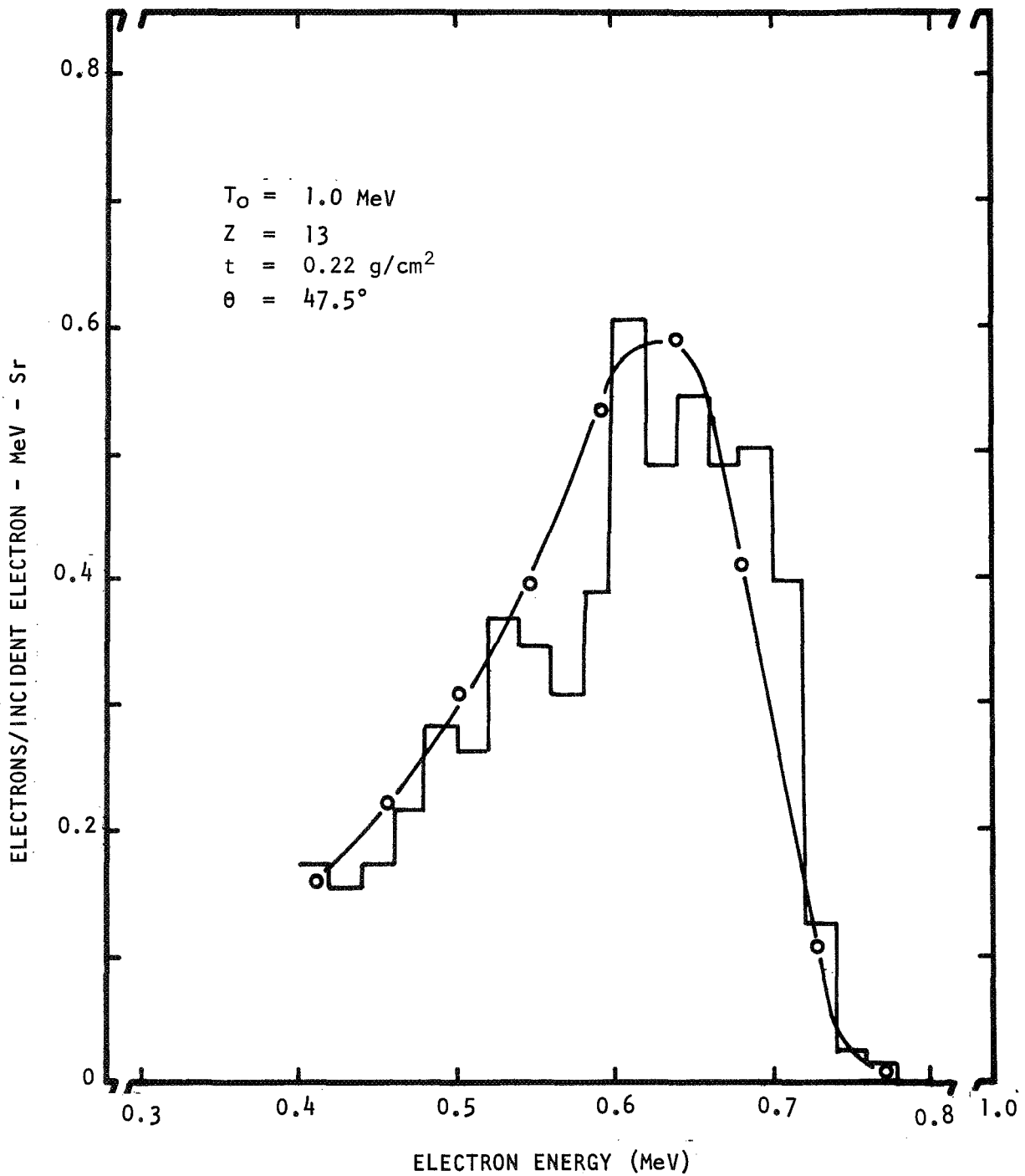


FIGURE 18. COMPARISON OF EXPERIMENTAL AND CALCULATED ELECTRON TRANSMISSION SPECTRA. THE CALCULATED SPECTRUM IS SHOWN IN HISTOGRAM FORM.



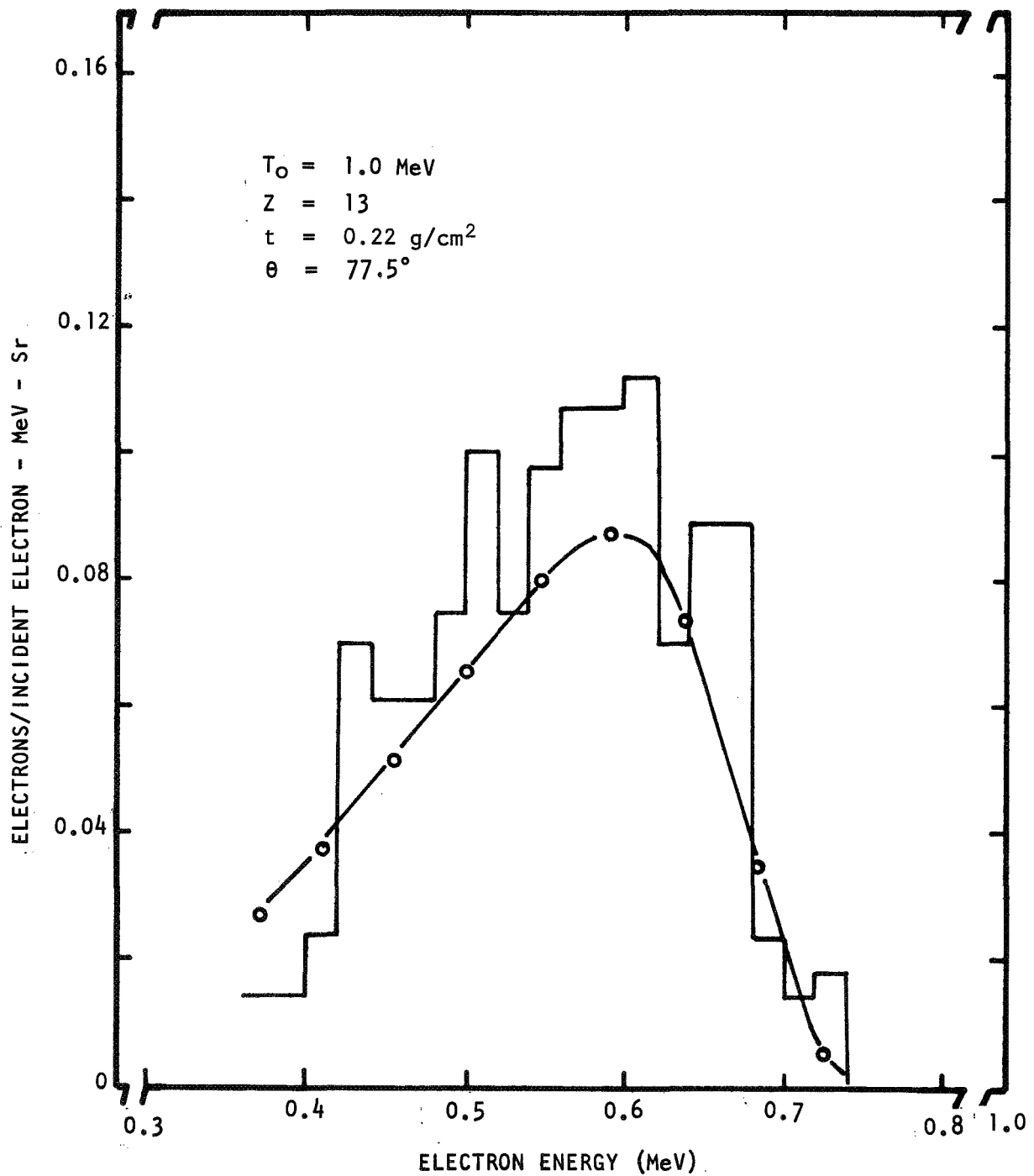


FIGURE 19. COMPARISON OF EXPERIMENTAL AND CALCULATED ELECTRON TRANSMISSION SPECTRA. THE CALCULATED SPECTRUM IS SHOWN IN HISTOGRAM FORM.

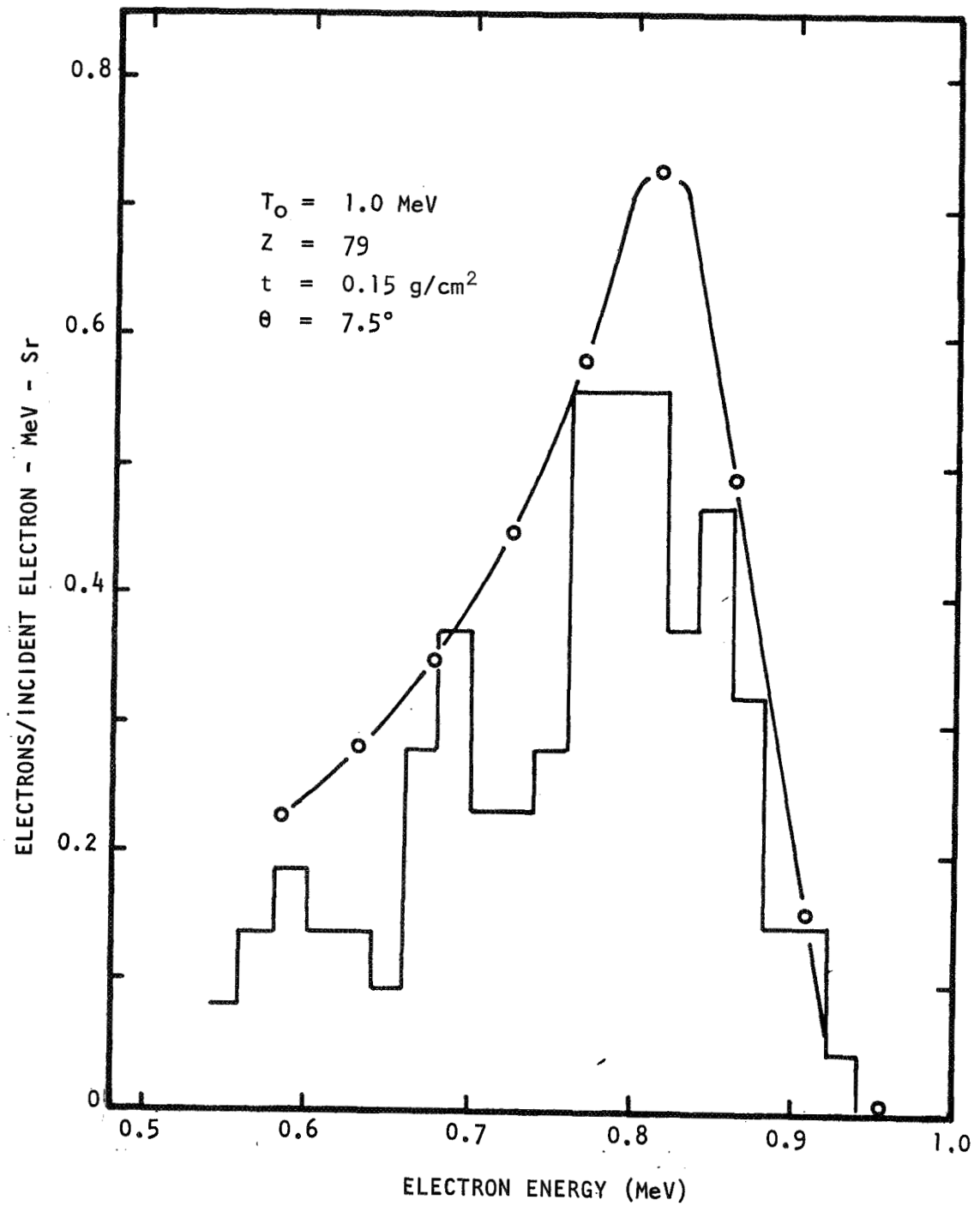


FIGURE 20. COMPARISON OF EXPERIMENTAL AND CALCULATED ELECTRON TRANSMISSION SPECTRA. THE CALCULATED SPECTRUM IS SHOWN IN HISTOGRAM FORM.

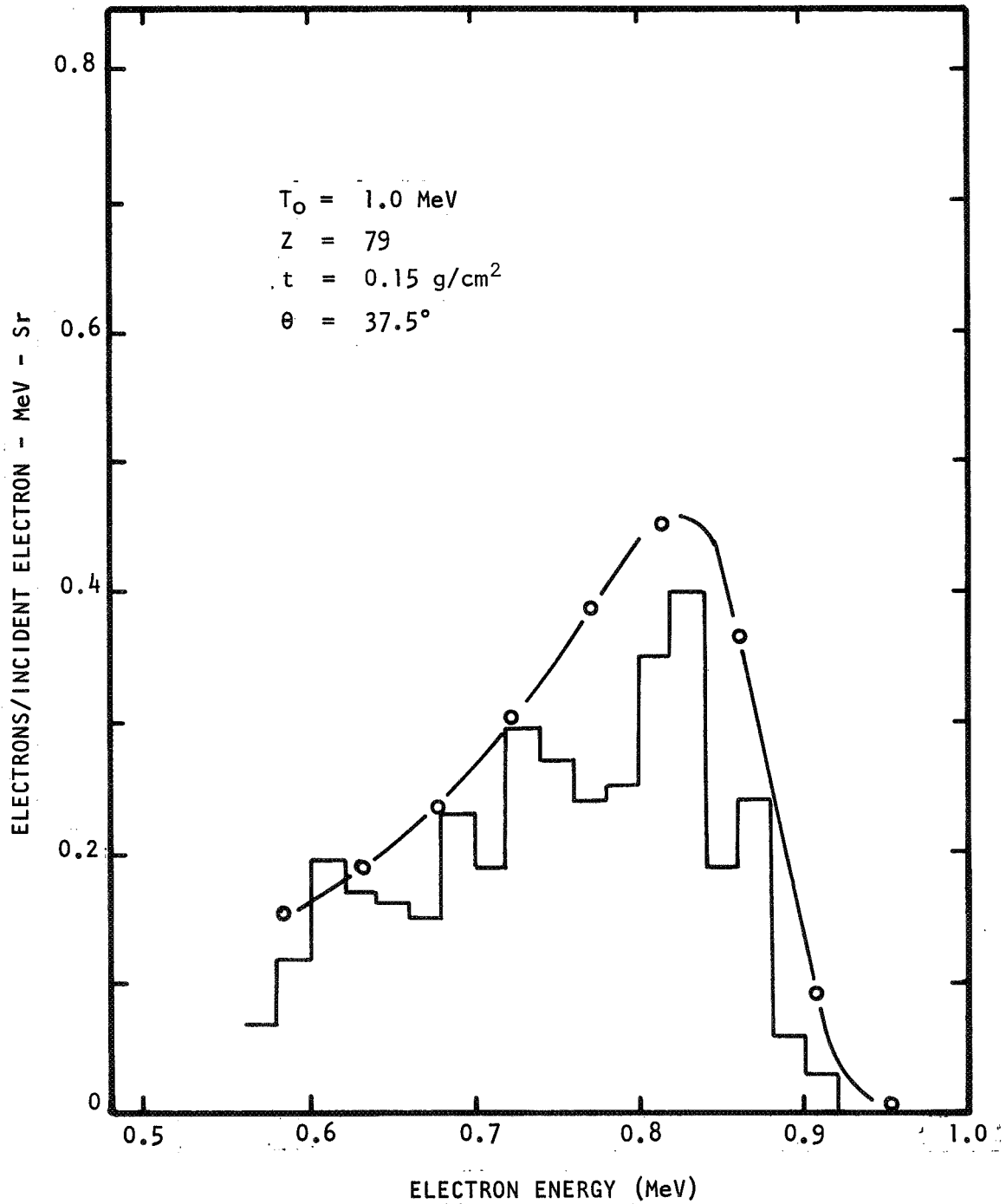


FIGURE 21. COMPARISON OF EXPERIMENTAL AND CALCULATED ELECTRON TRANSMISSION SPECTRA. THE CALCULATED SPECTRUM IS SHOWN IN HISTOGRAM FORM.

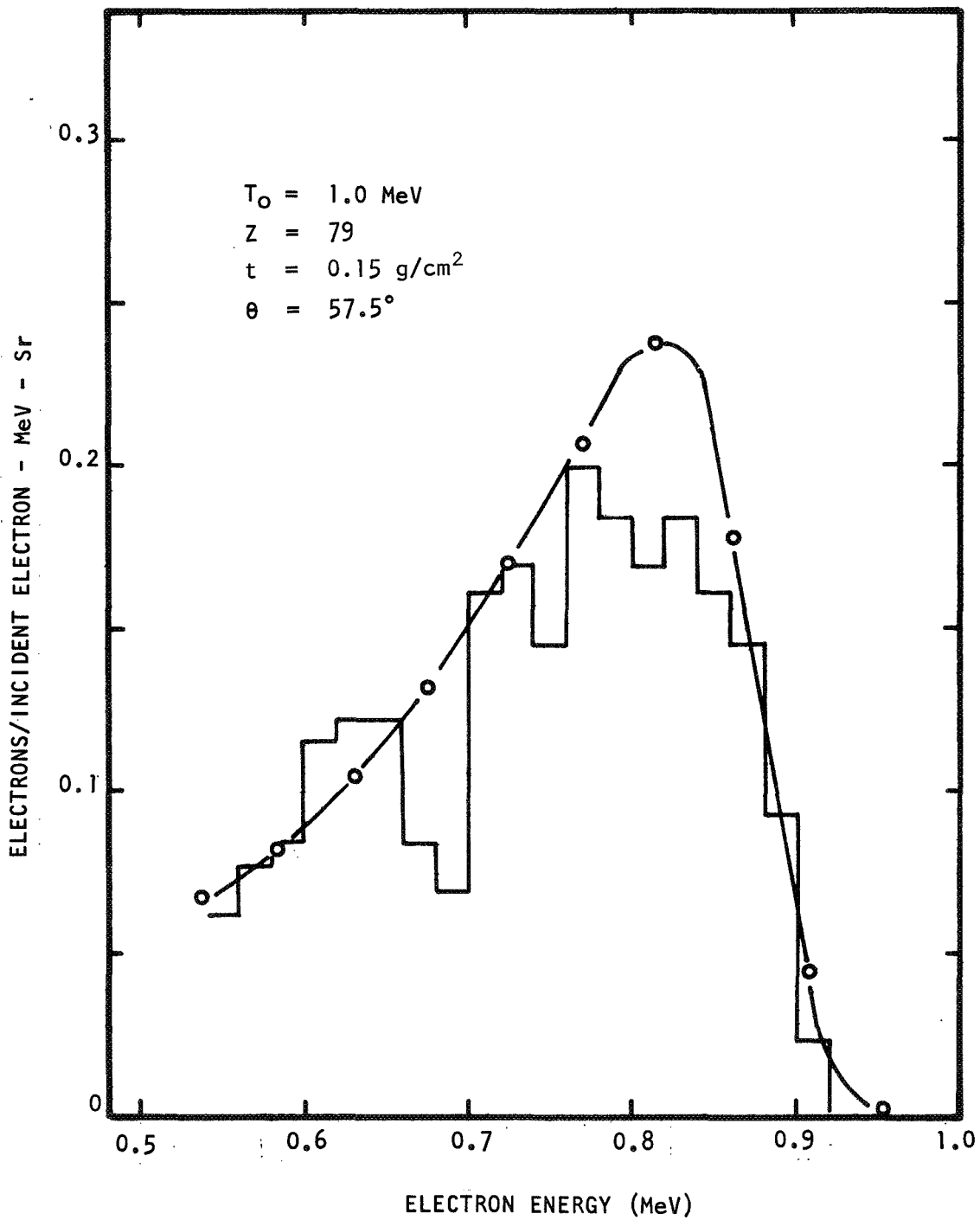


FIGURE 22. COMPARISON OF EXPERIMENTAL AND CALCULATED ELECTRON TRANSMISSION SPECTRA. THE CALCULATED SPECTRUM IS SHOWN IN HISTOGRAM FORM.

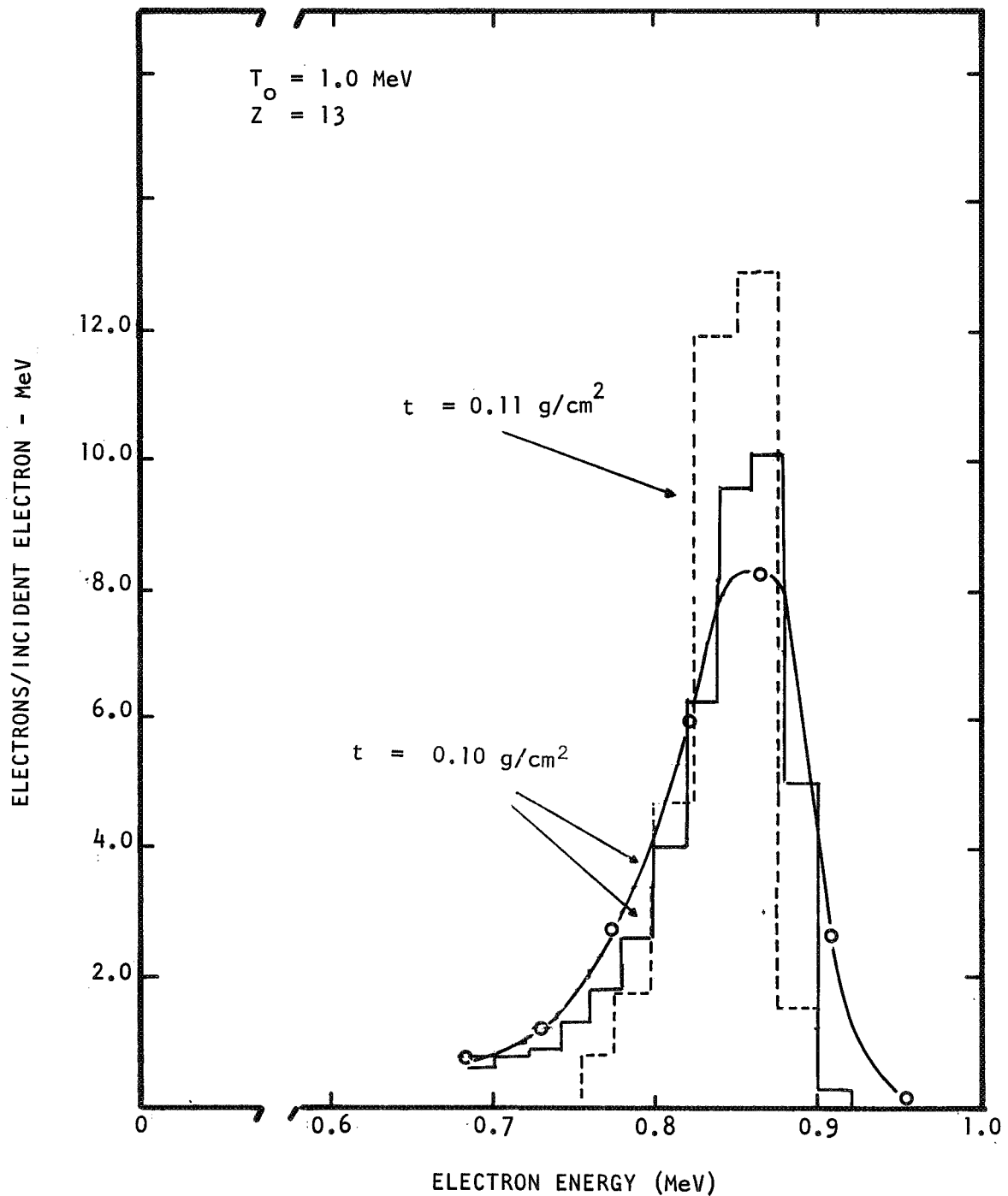


FIGURE 23. COMPARISON OF EXPERIMENTAL AND CALCULATED TOTAL TRANSMISSION SPECTRA. SOLID HISTOGRAM IS THE CALCULATED SPECTRUM FROM ETRAN-15. DASHED HISTOGRAM IS FROM AN EARLIER COMPARISON.

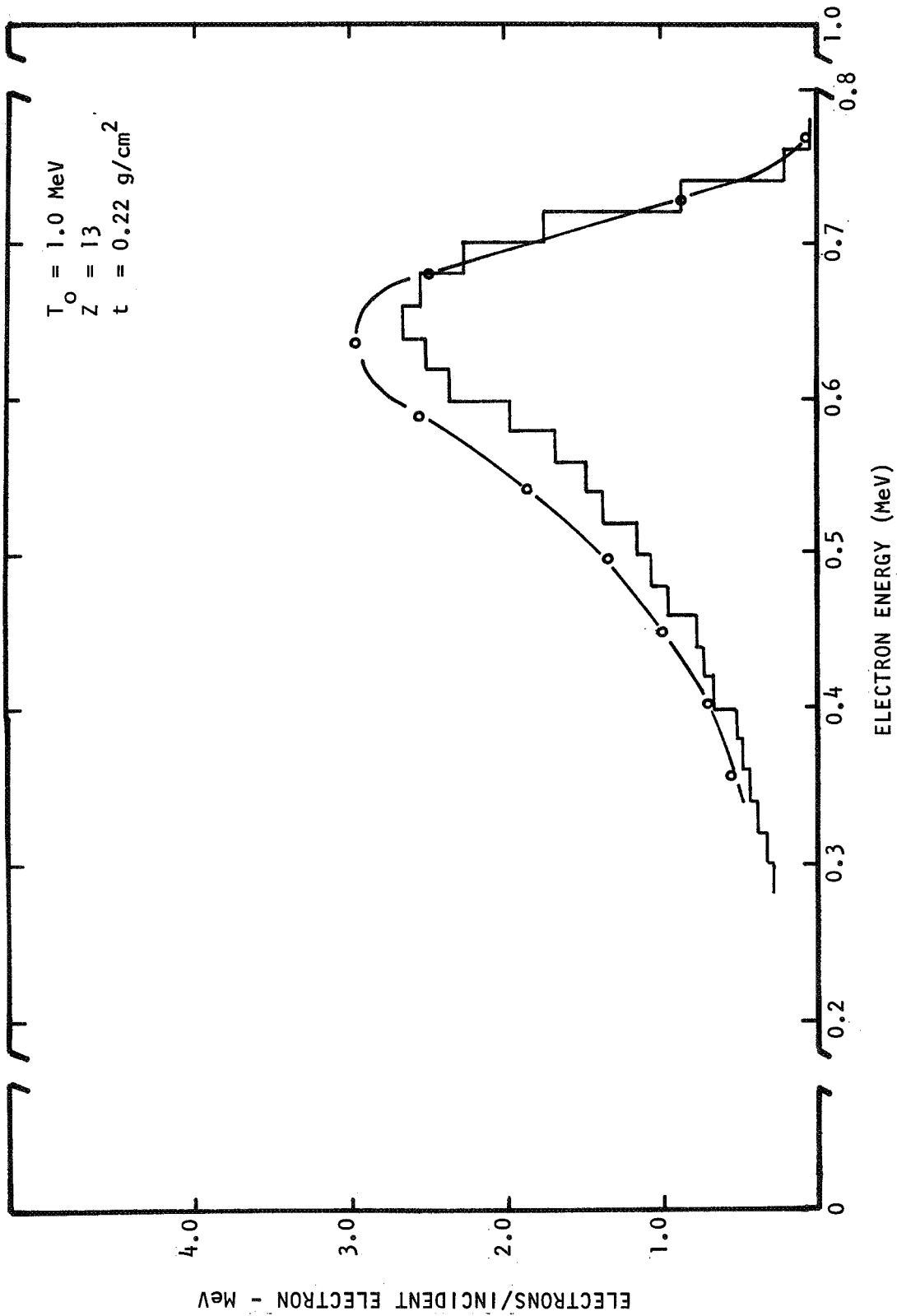


FIGURE 24. COMPARISON OF EXPERIMENTAL AND CALCULATED TOTAL TRANSMISSION SPECTRA. THE CALCULATED SPECTRUM IS SHOWN IN HISTOGRAM FORM.



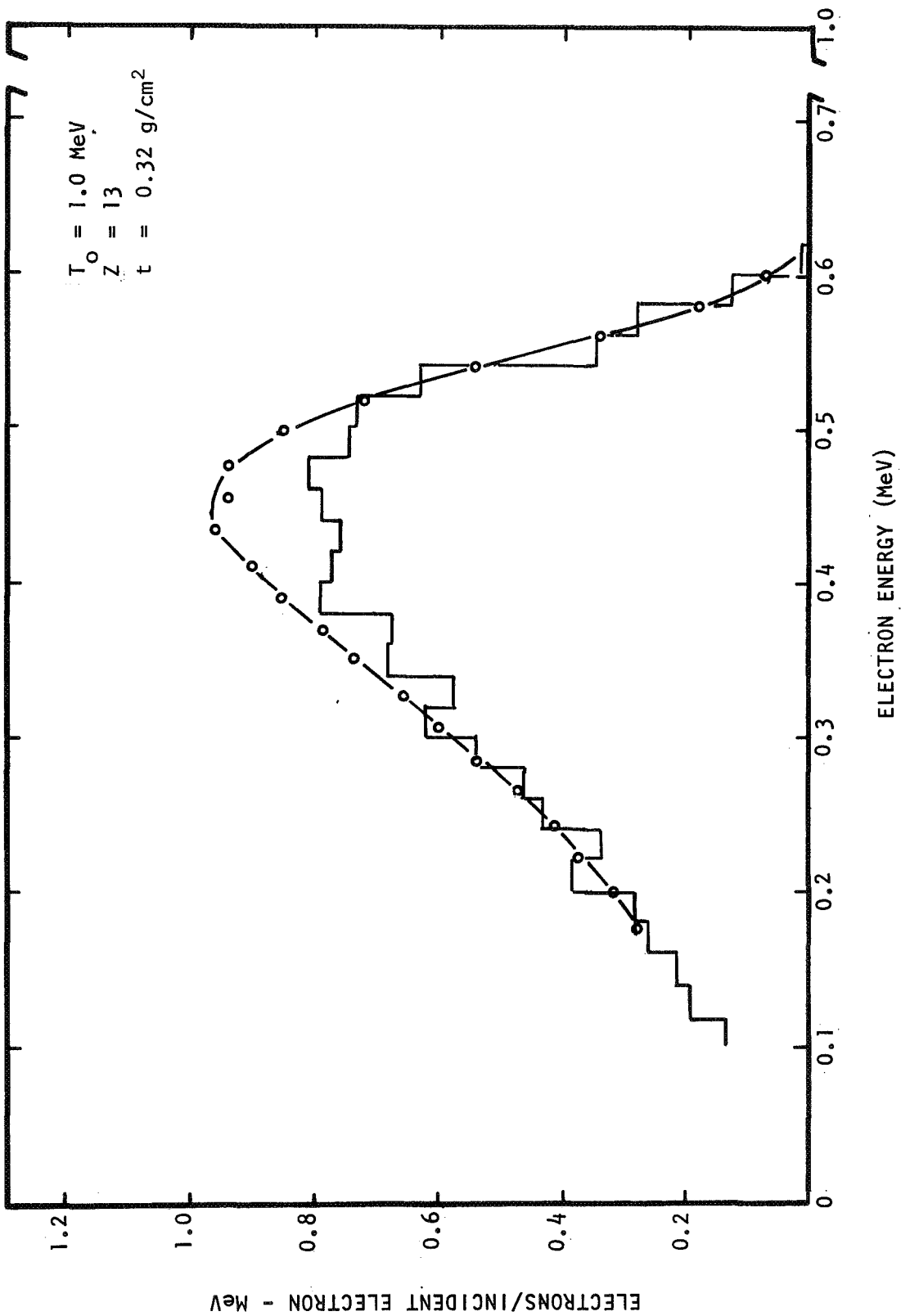


FIGURE 25. COMPARISON OF EXPERIMENTAL AND CALCULATED TOTAL TRANSMISSION SPECTRA. THE CALCULATED SPECTRUM IS SHOWN IN HISTOGRAM FORM.

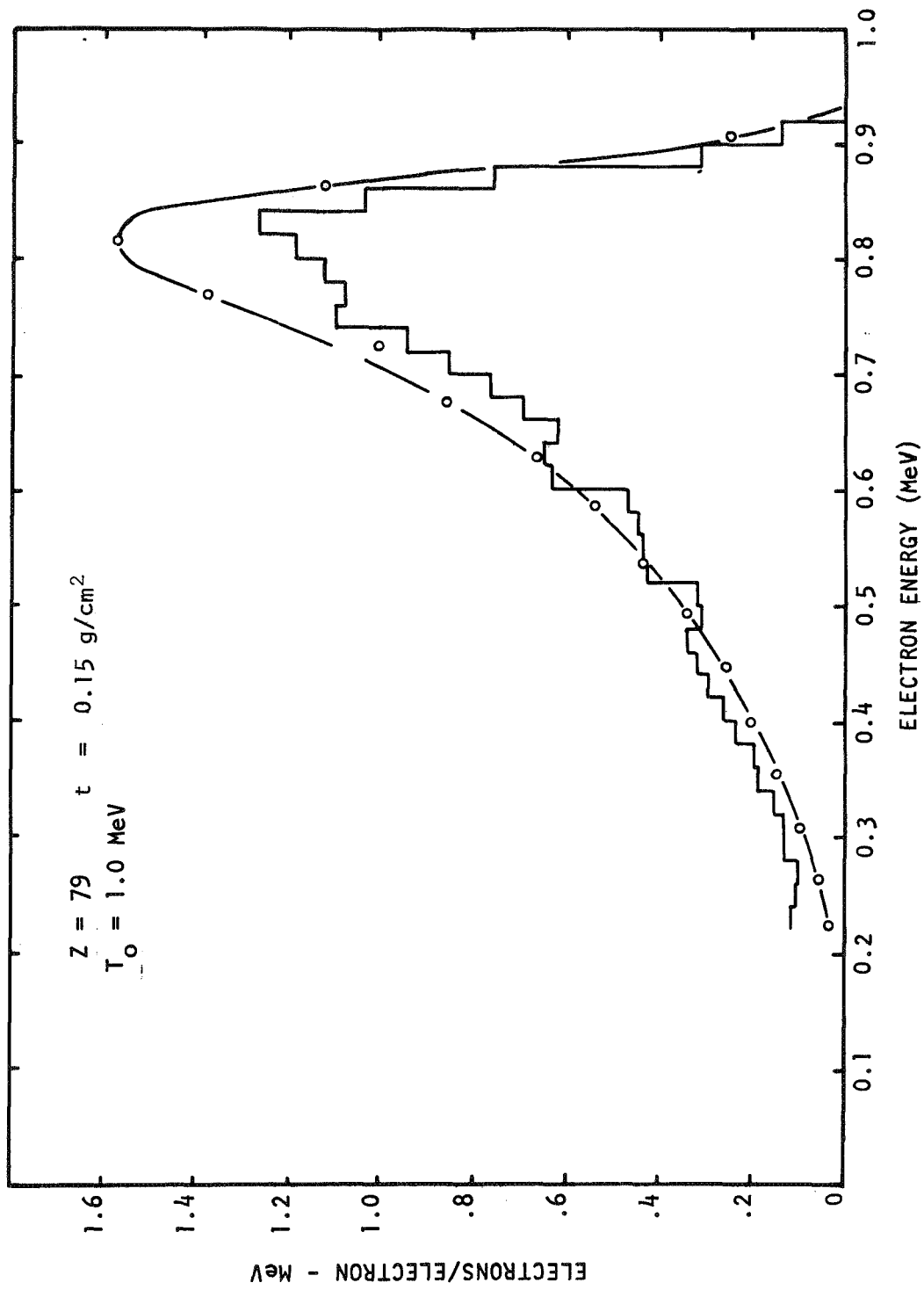


FIGURE 26. COMPARISON OF EXPERIMENTAL AND CALCULATED TOTAL TRANSMISSION SPECTRA. THE CALCULATED SPECTRUM IS SHOWN IN HISTOGRAM FORM.

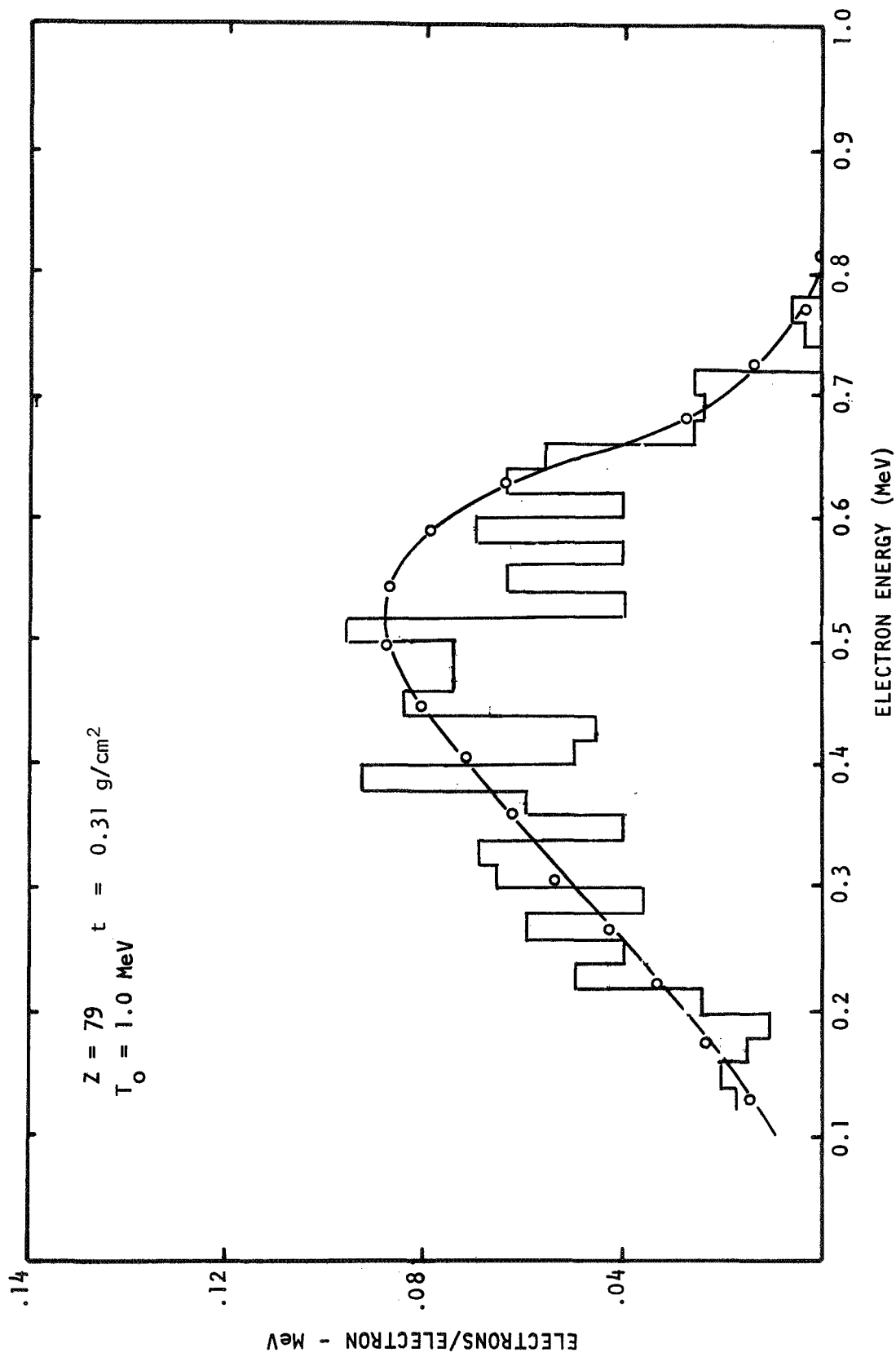


FIGURE 27. COMPARISON OF EXPERIMENTAL AND CALCULATED TOTAL TRANSMISSION SPECTRA. THE CALCULATED SPECTRUM IS SHOWN IN HISTOGRAM FORM.

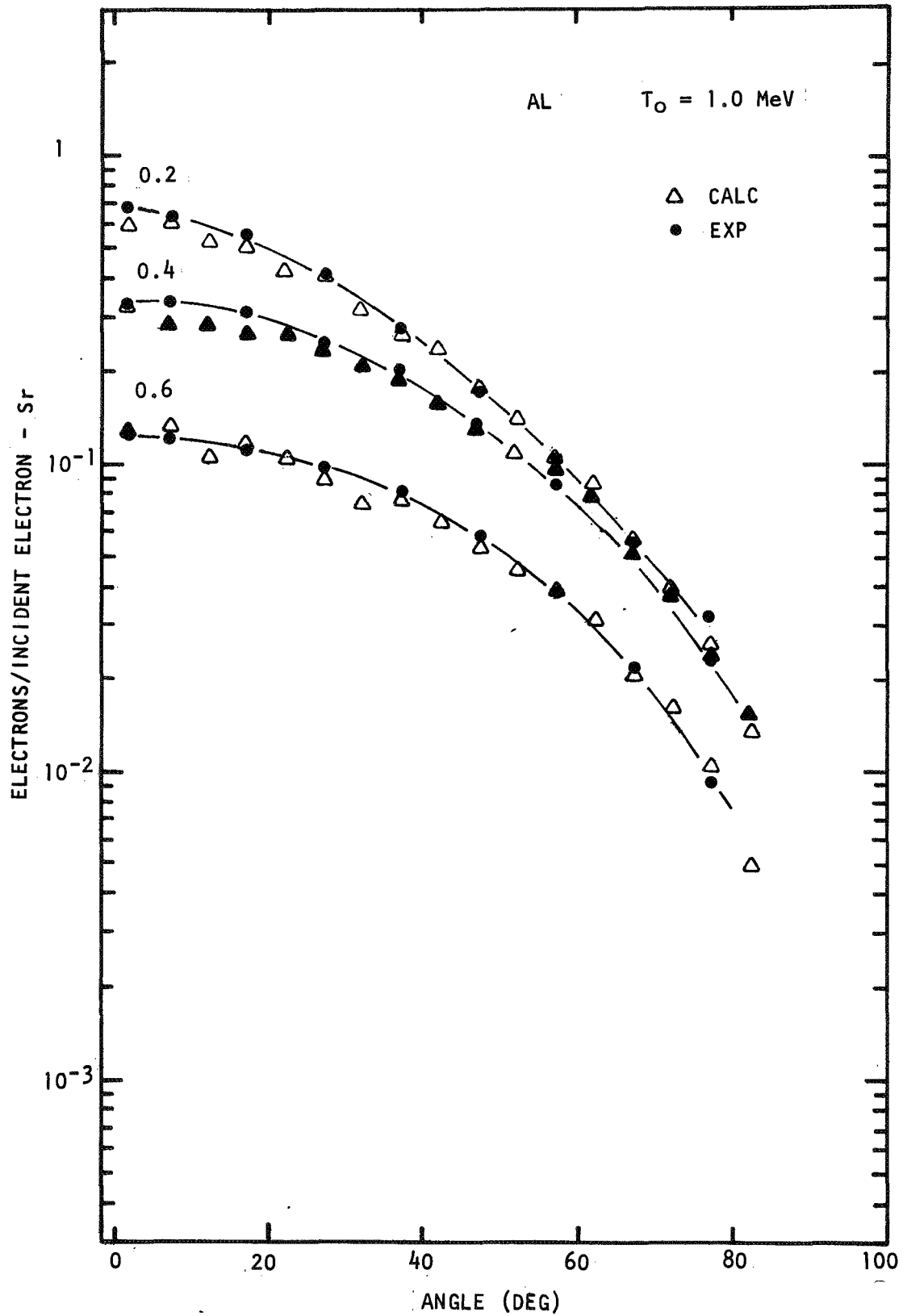


FIGURE 28. COMPARISON OF MONTE CARLO AND EXPERIMENTAL ANGULAR DISTRIBUTIONS OF TRANSMITTED ELECTRONS FOR AL TARGETS OF 0.2, 0.4 AND 0.6 THE RANGE AT 1.0 MeV.

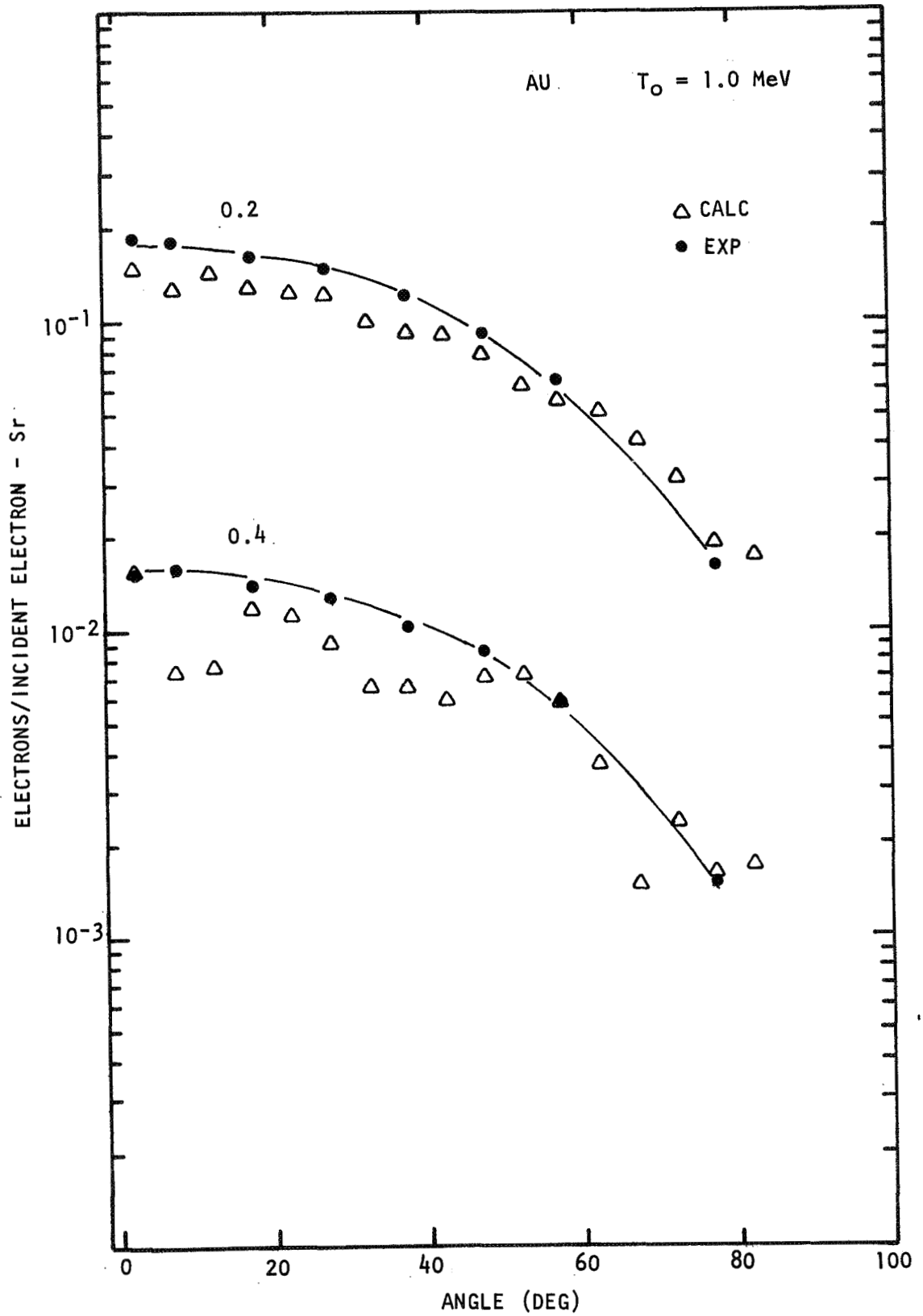


FIGURE 29. COMPARISON OF MONTE CARLO AND EXPERIMENTAL ANGULAR DISTRIBUTIONS OF TRANSMITTED ELECTRONS FOR Au TARGETS OF 0.2 AND 0.4 THE RANGE AT 1.0 MeV.

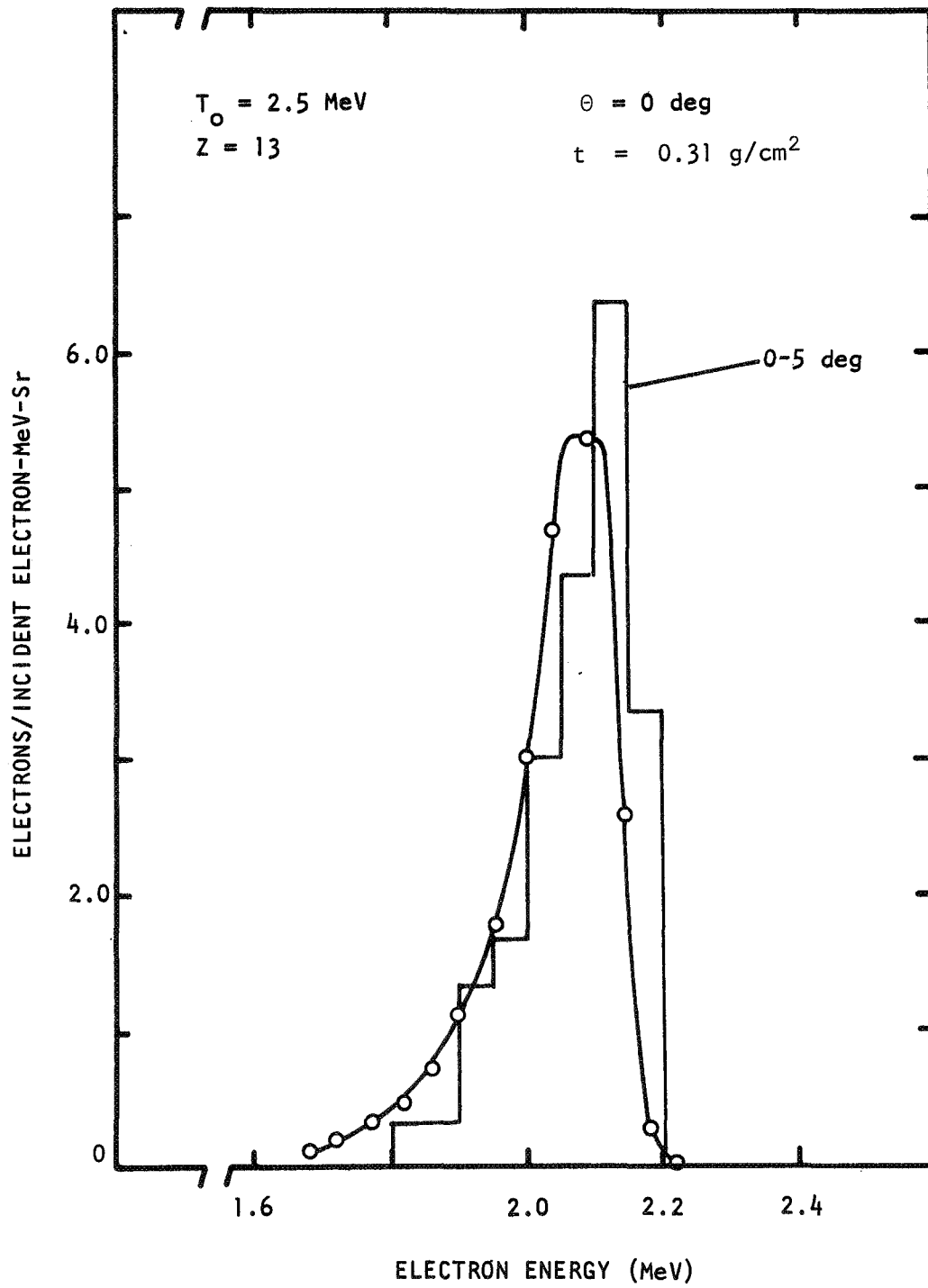


FIGURE 30. COMPARISON OF EXPERIMENTAL AND CALCULATED ELECTRON TRANSMISSION SPECTRA. THE CALCULATED SPECTRUM IS SHOWN IN HISTOGRAM FORM.

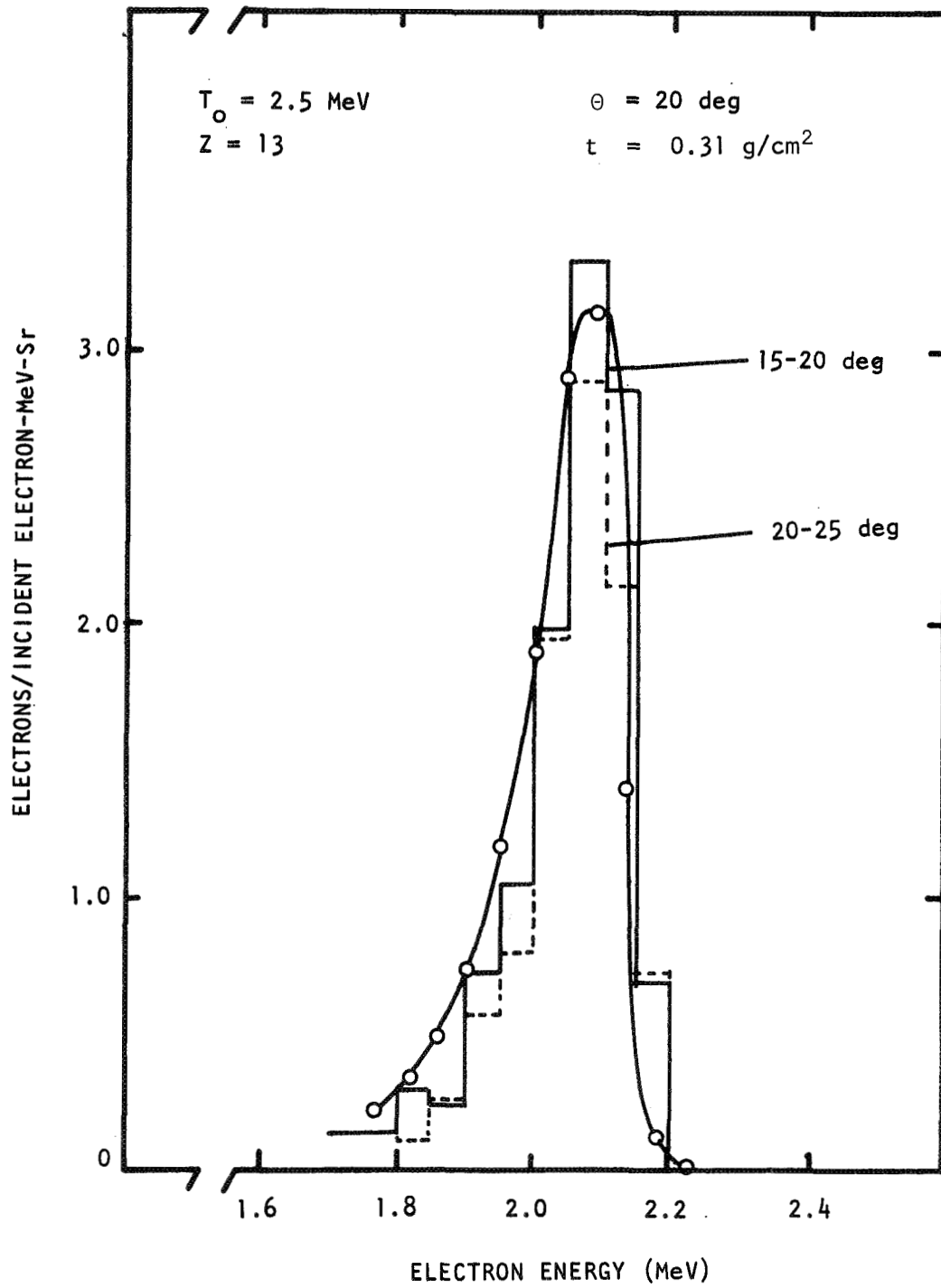


FIGURE 31. COMPARISON OF EXPERIMENTAL AND CALCULATED ELECTRON TRANSMISSION SPECTRA. THE CALCULATED SPECTRA ARE SHOWN IN HISTOGRAM FORM.

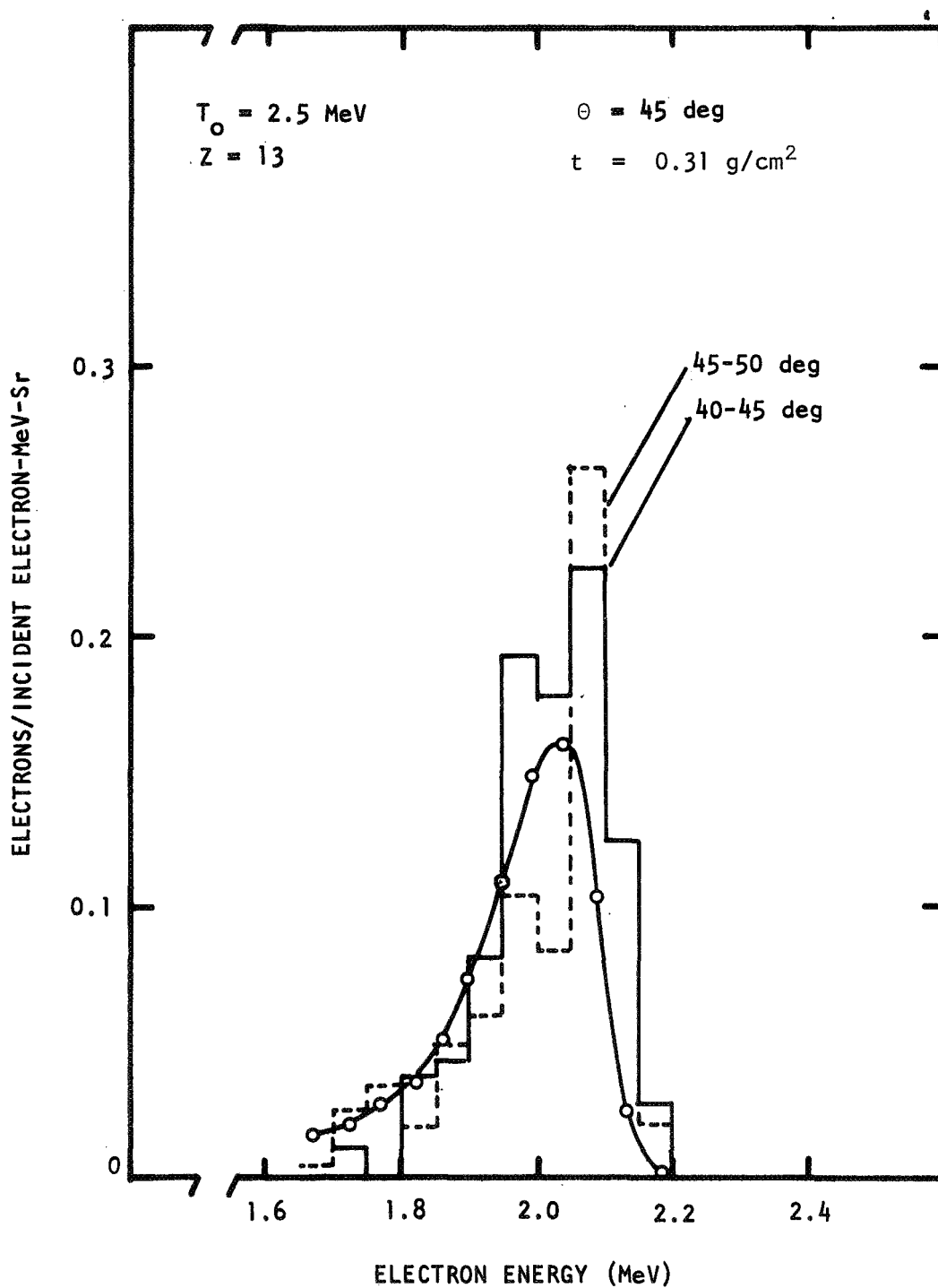


FIGURE 32. COMPARISON OF EXPERIMENTAL AND CALCULATED ELECTRON TRANSMISSION SPECTRA. THE CALCULATED SPECTRA ARE SHOWN IN HISTOGRAM FORM.



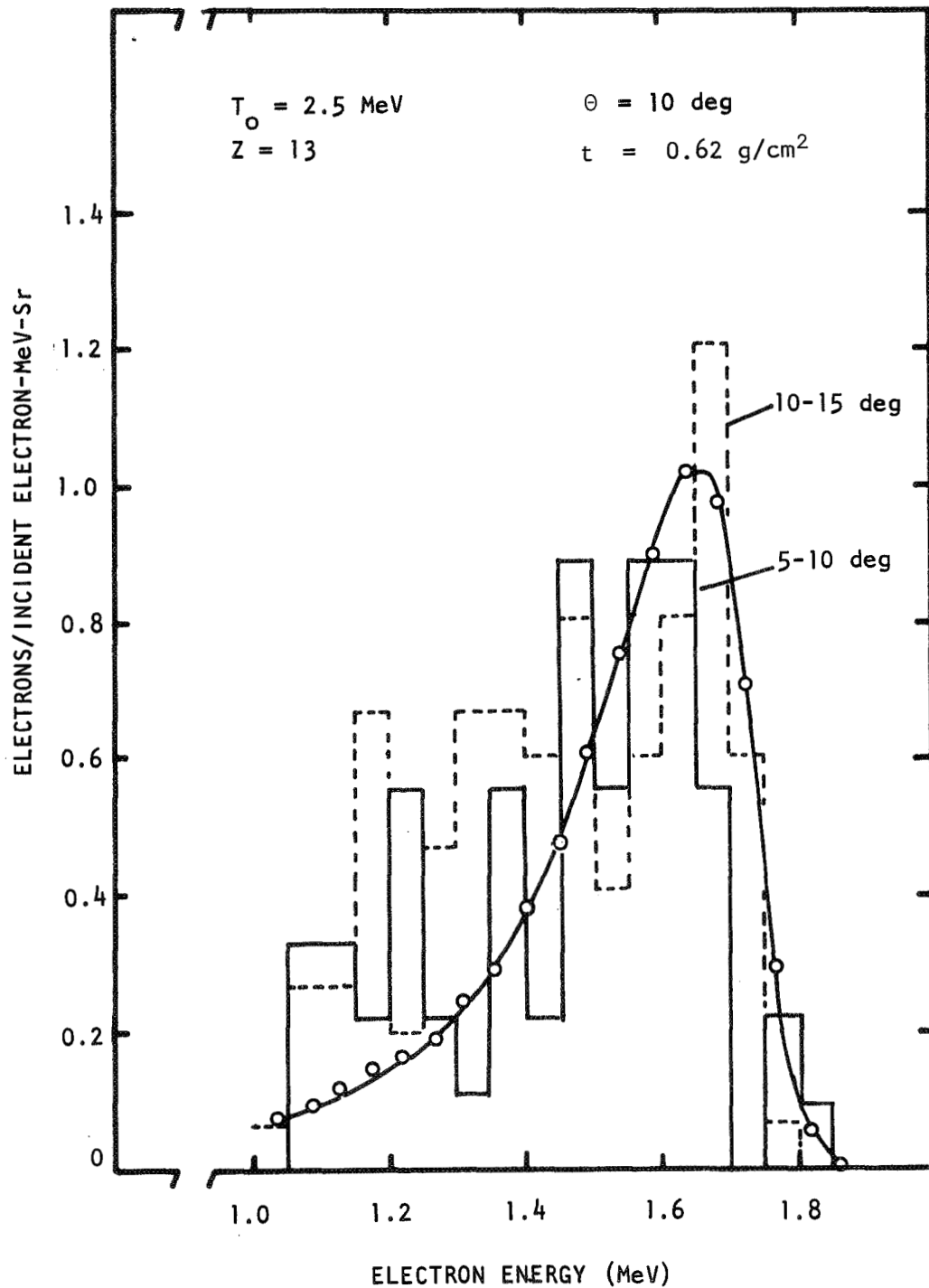


FIGURE 33. COMPARISON OF EXPERIMENTAL AND CALCULATED ELECTRON TRANSMISSION SPECTRA. THE CALCULATED SPECTRA ARE SHOWN IN HISTOGRAM FORM.

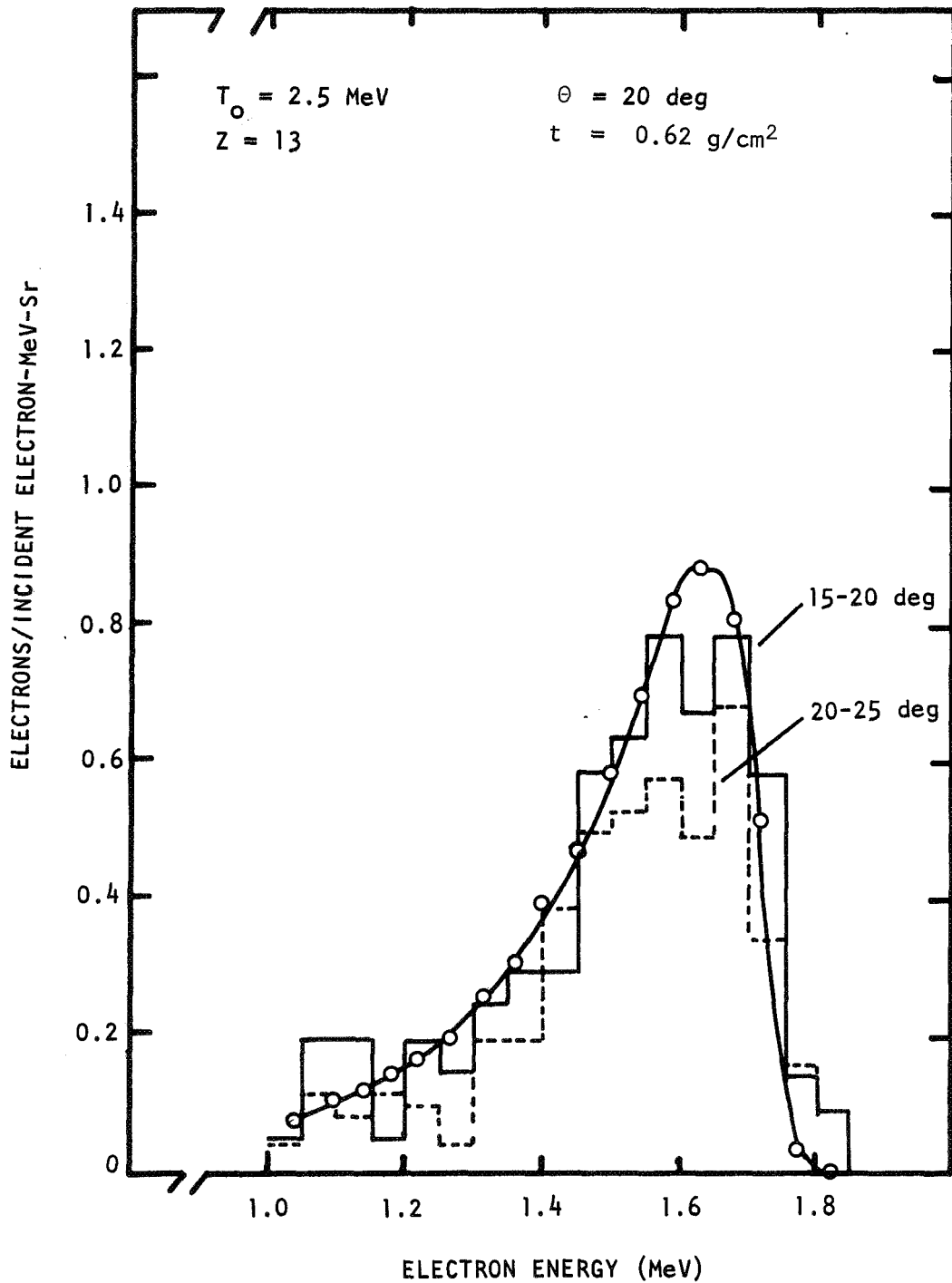


FIGURE 34. COMPARISON OF EXPERIMENTAL AND CALCULATED ELECTRON TRANSMISSION SPECTRA. THE CALCULATED SPECTRA ARE SHOWN IN HISTOGRAM FORM.

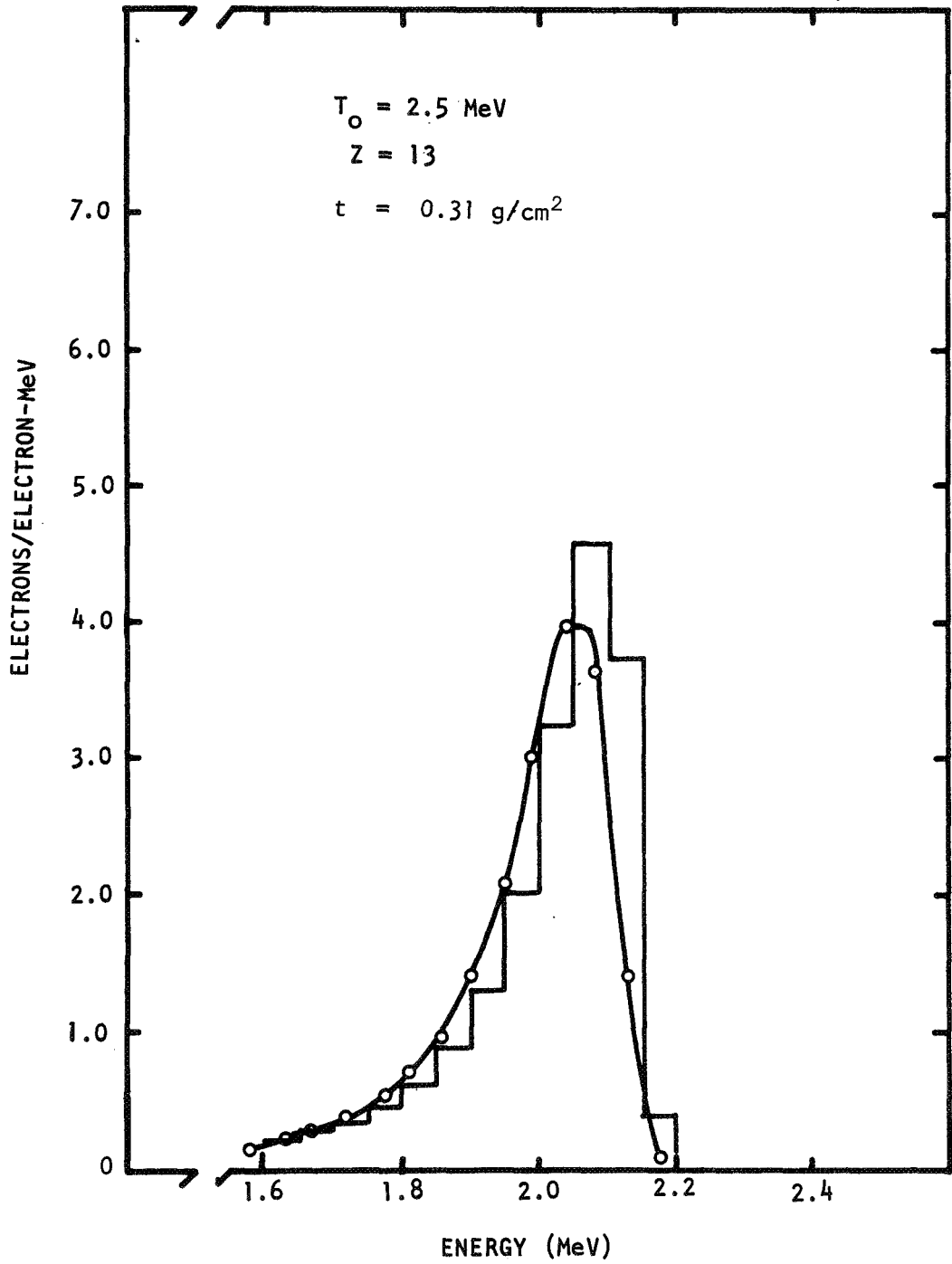


FIGURE 35. COMPARISON OF EXPERIMENTAL AND CALCULATED TOTAL TRANSMISSION. THE CALCULATED SPECTRUM IS SHOWN IN HISTOGRAM FORM.

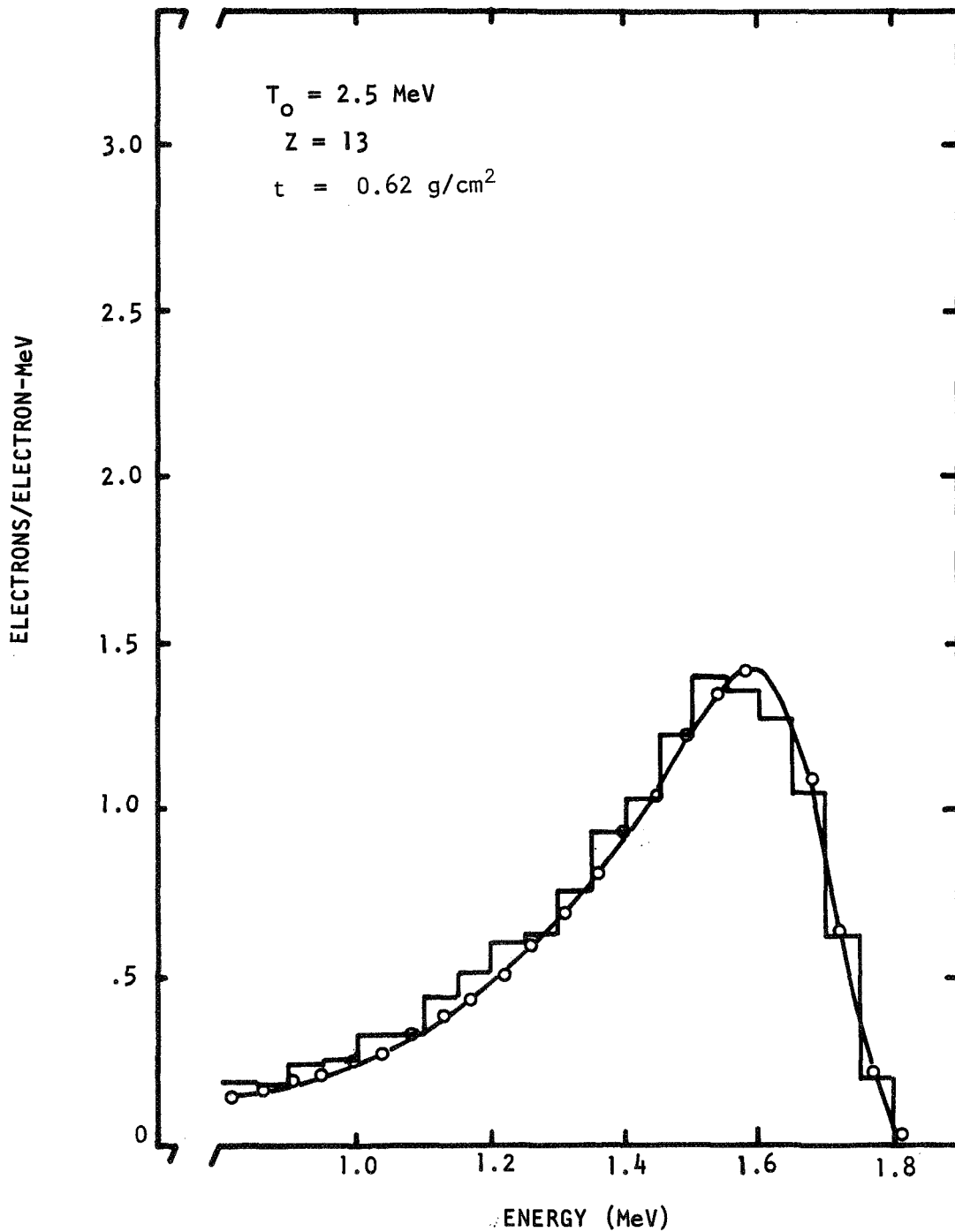


FIGURE 36. COMPARISON OF EXPERIMENTAL AND CALCULATED TOTAL TRANSMISSION. THE CALCULATED SPECTRUM IS SHOWN IN HISTOGRAM FORM.

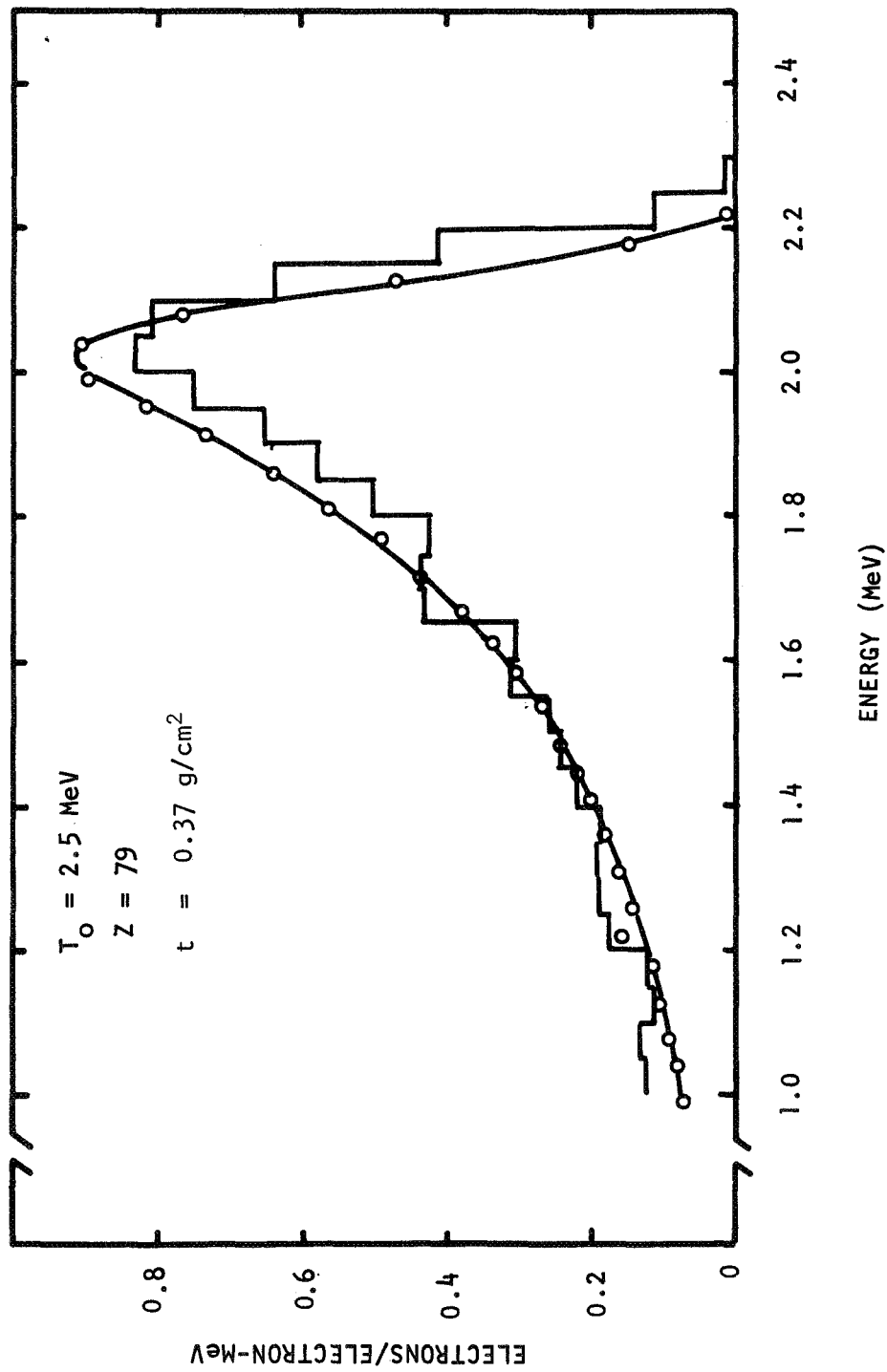


FIGURE 37. COMPARISON OF EXPERIMENTAL AND CALCULATED TOTAL TRANSMISSION. THE CALCULATED SPECTRUM IS SHOWN IN HISTOGRAM FORM.

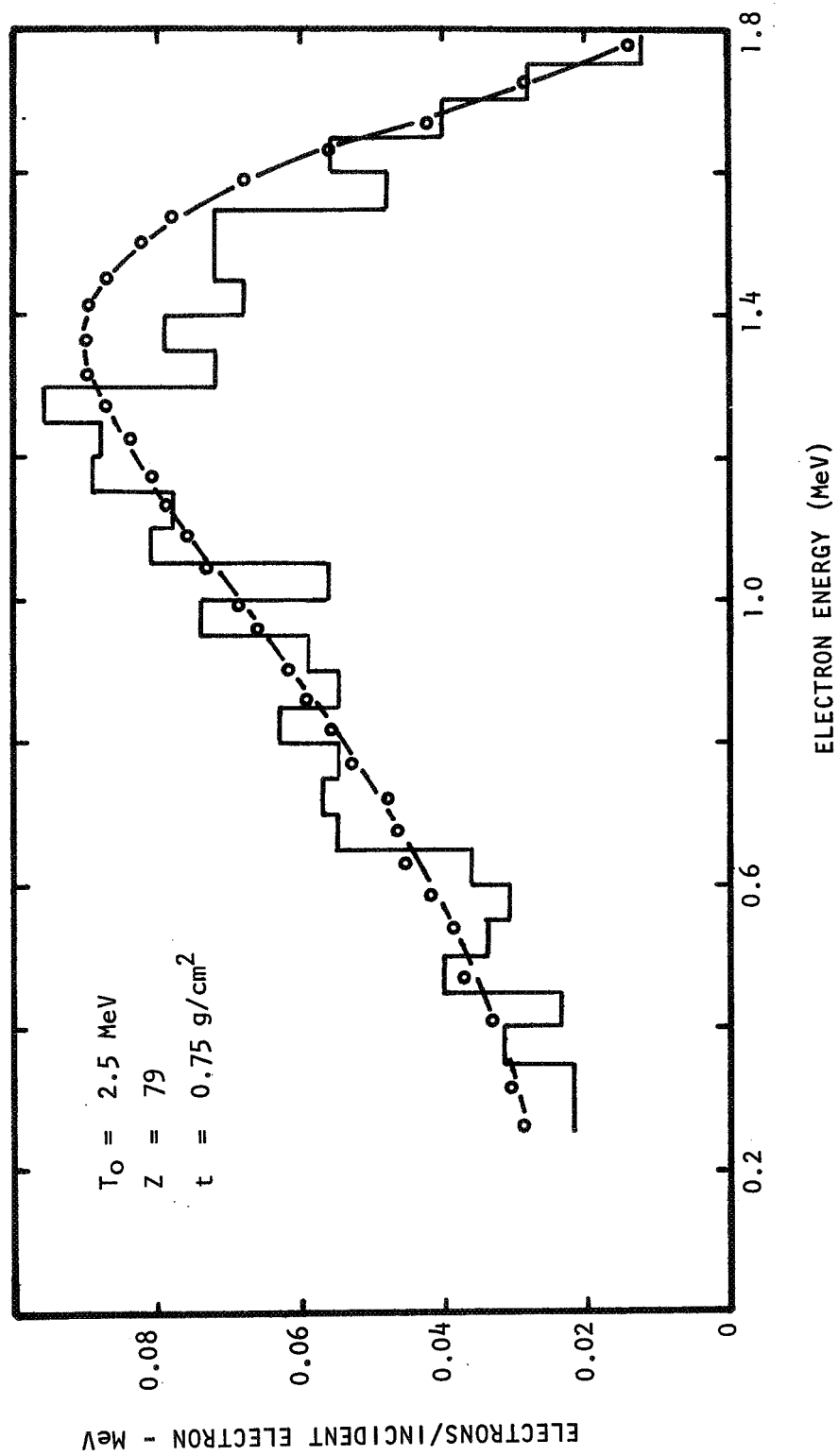


FIGURE 38. COMPARISON OF EXPERIMENTAL AND CALCULATED TOTAL TRANSMISSION. THE CALCULATED SPECTRUM IS SHOWN IN HISTOGRAM FORM.

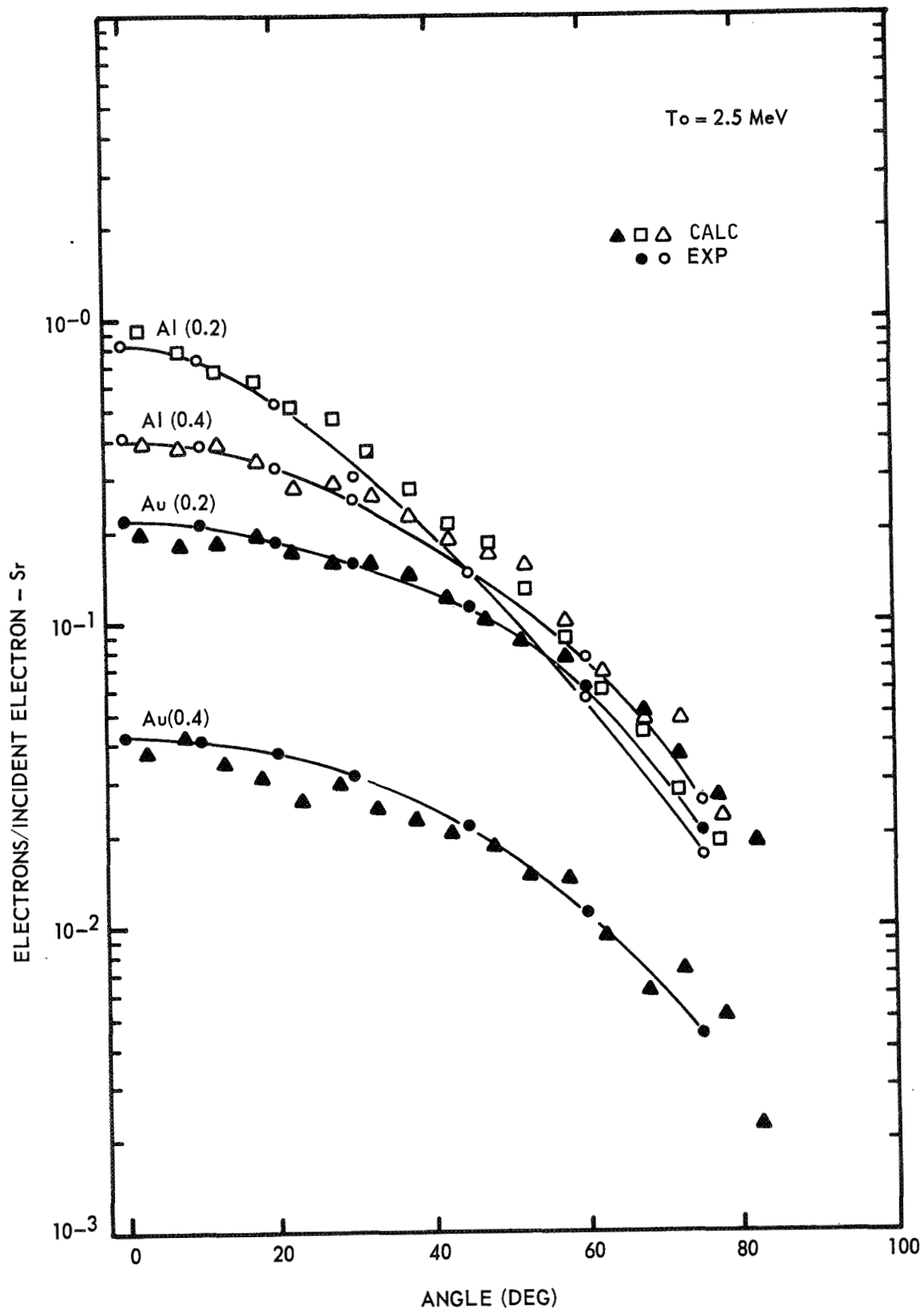


FIGURE 39. COMPARISON OF MONTE CARLO AND EXPERIMENTAL ANGULAR DISTRIBUTIONS OF TRANSMITTED ELECTRONS FOR Al AND Au TARGETS OF 0.2 AND 0.4 THE RANGE AT 2.5 MeV.

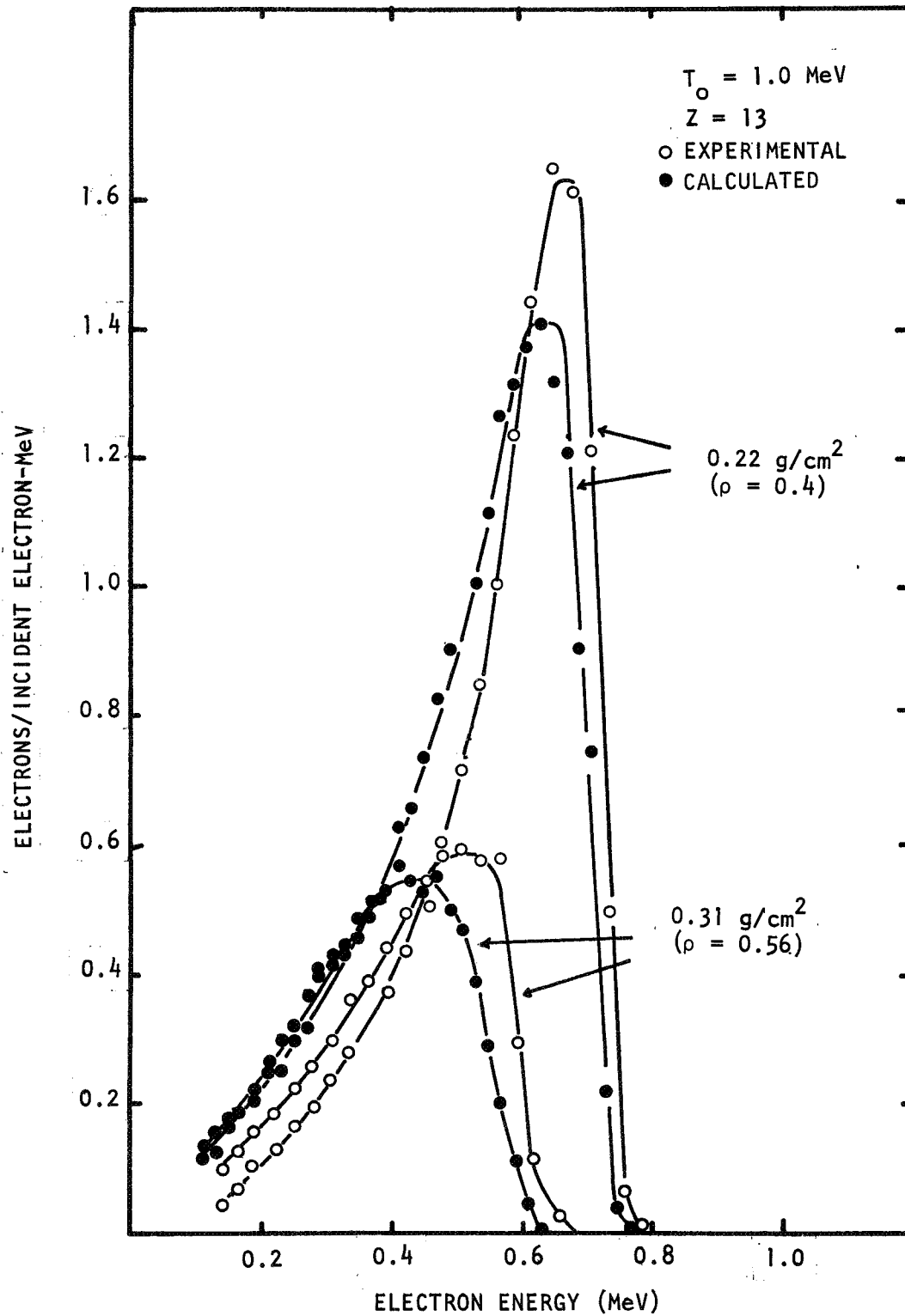


FIGURE 40. COMPARISON OF EXPERIMENTAL AND CALCULATED TOTAL TRANSMISSION SPECTRA FOR AN INCIDENT, COSINE-LAW FLUX.



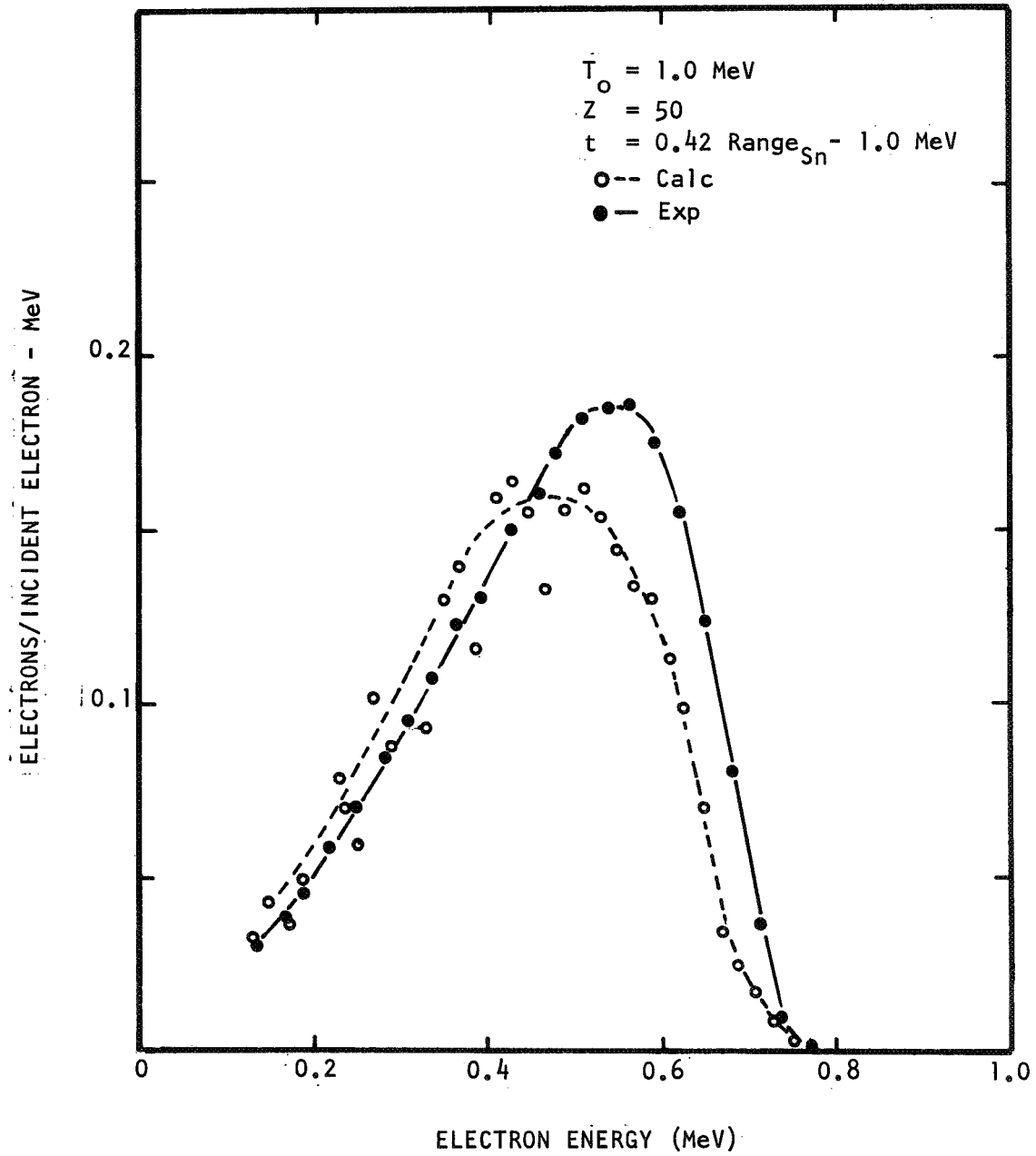


FIGURE 41. COMPARISON OF EXPERIMENTAL AND CALCULATED TOTAL TRANSMISSION SPECTRA FOR AN INCIDENT, COSINE-LAW FLUX.

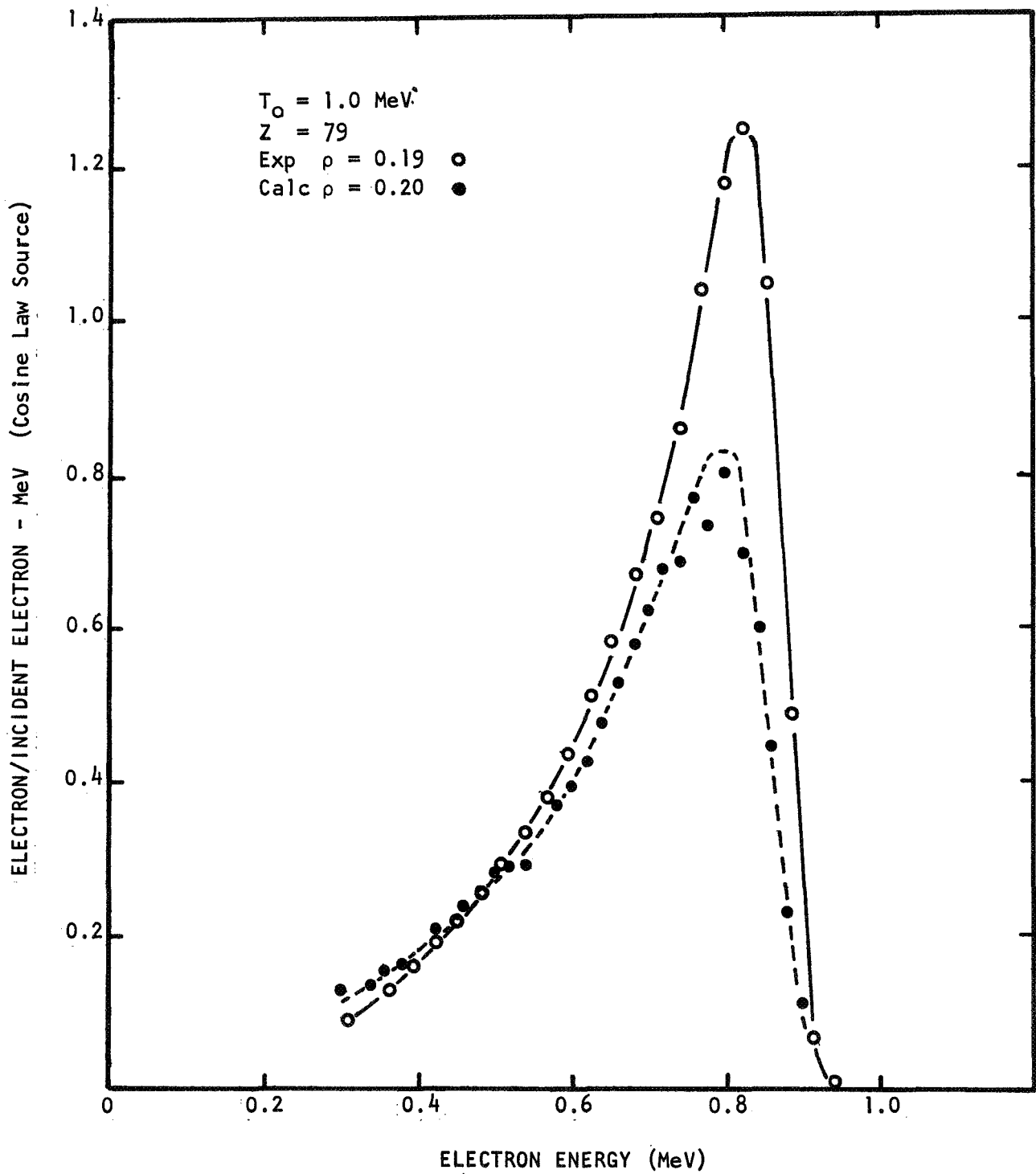


FIGURE 42. COMPARISON OF EXPERIMENTAL AND CALCULATED TOTAL TRANSMISSION SPECTRA FOR AN INCIDENT, COSINE-LAW FLUX.

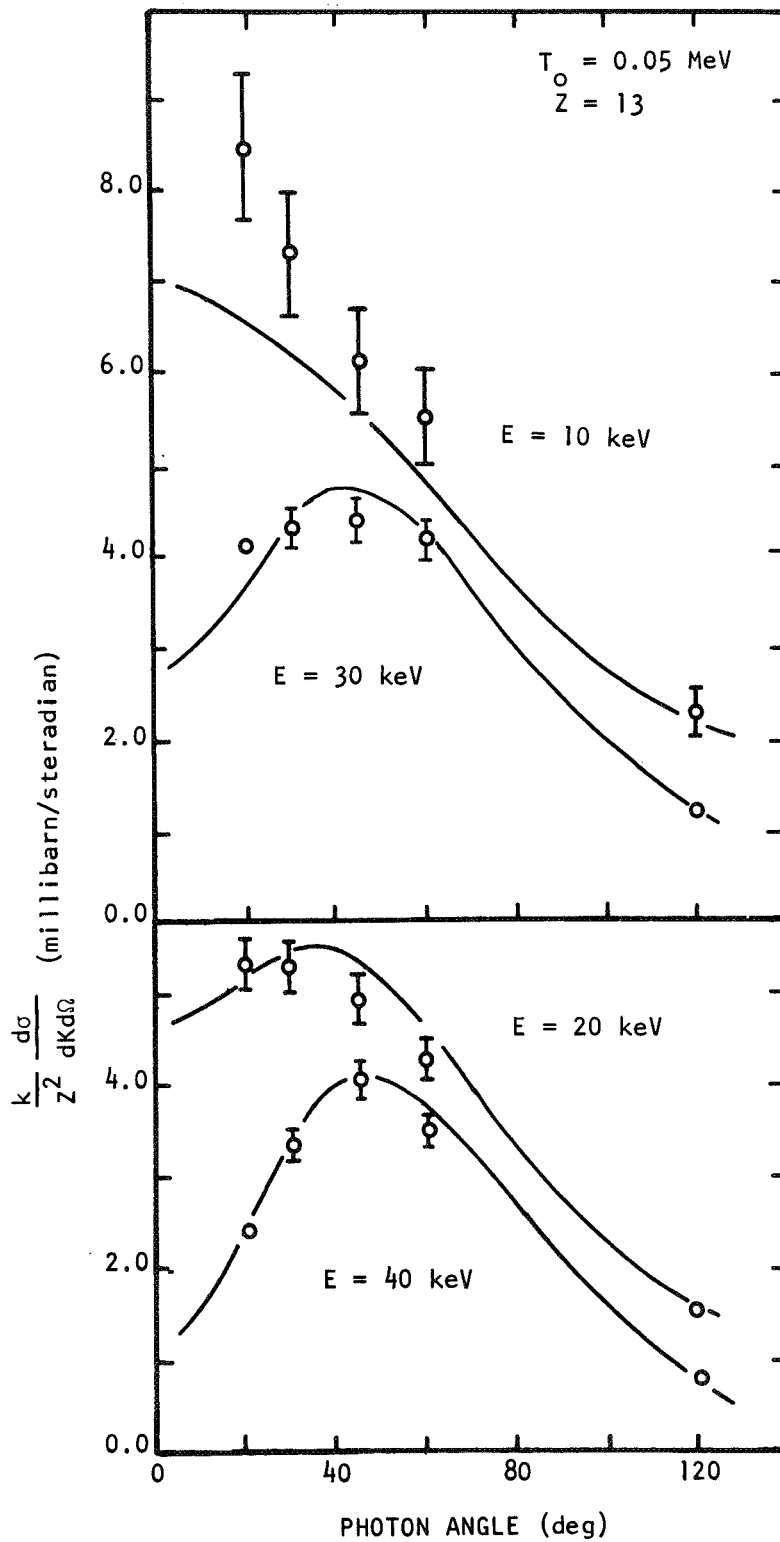


FIGURE 43. BREMSSTRAHLUNG CROSS SECTION VALUES FROM THE WORK OF BRYSK, ET AL (REF 8 ). EXPERIMENTAL VALUES ARE SHOWN AS POINTS.

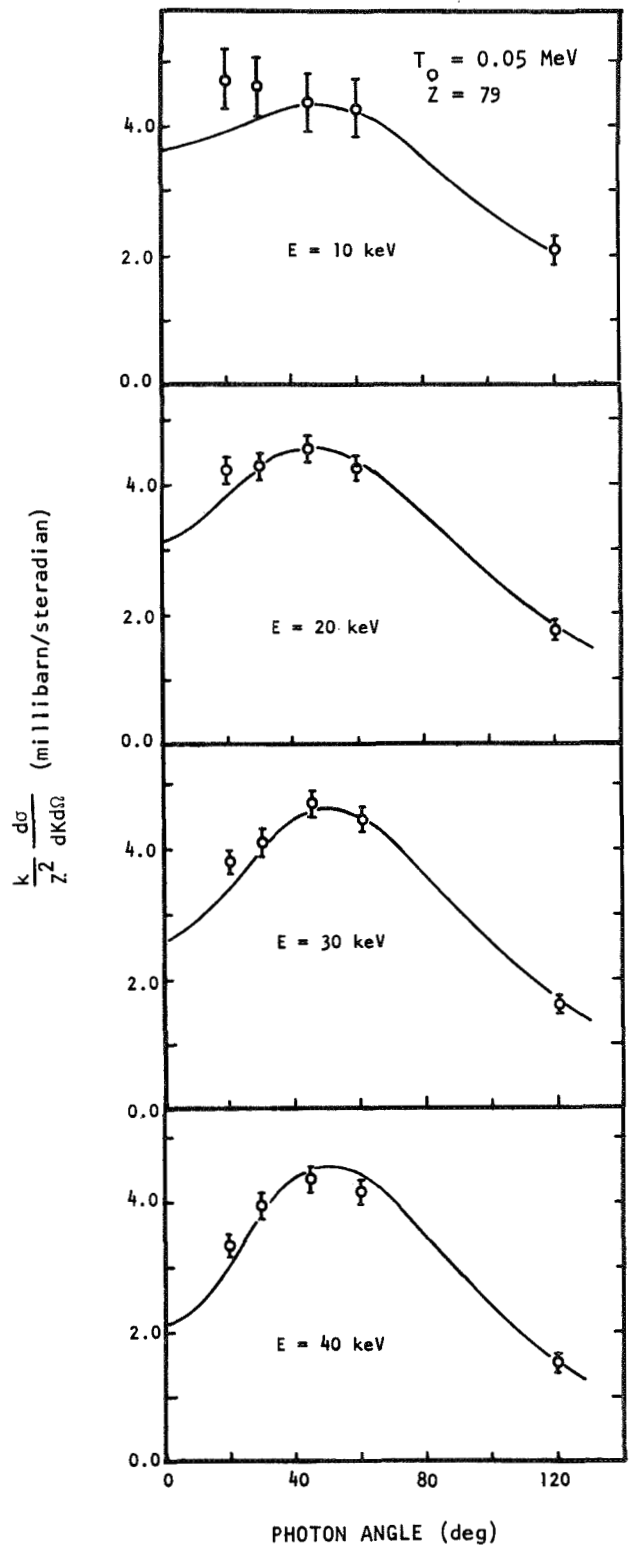


FIGURE 44. BREMSSTRAHLUNG CROSS SECTION VALUES FROM THE WORK OF BRYSK, ET AL (REF 8 ). EXPERIMENTAL VALUES ARE SHOWN AS POINTS.

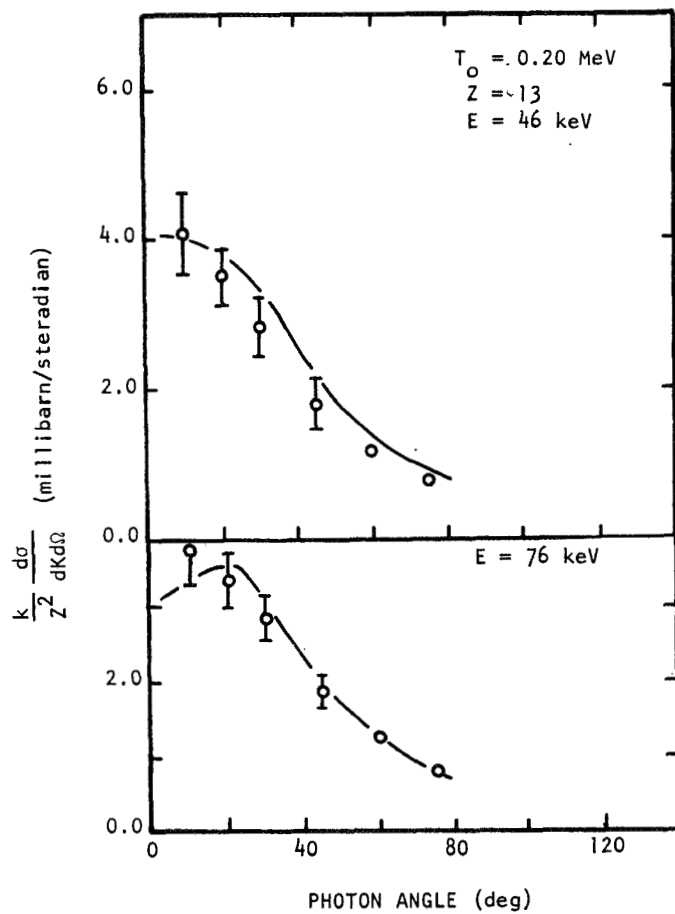


FIGURE 45. BREMSSTRAHLUNG CROSS SECTION VALUES FROM THE WORK OF BRYSK, ET AL. EXPERIMENTAL VALUES ARE SHOWN AS POINTS.

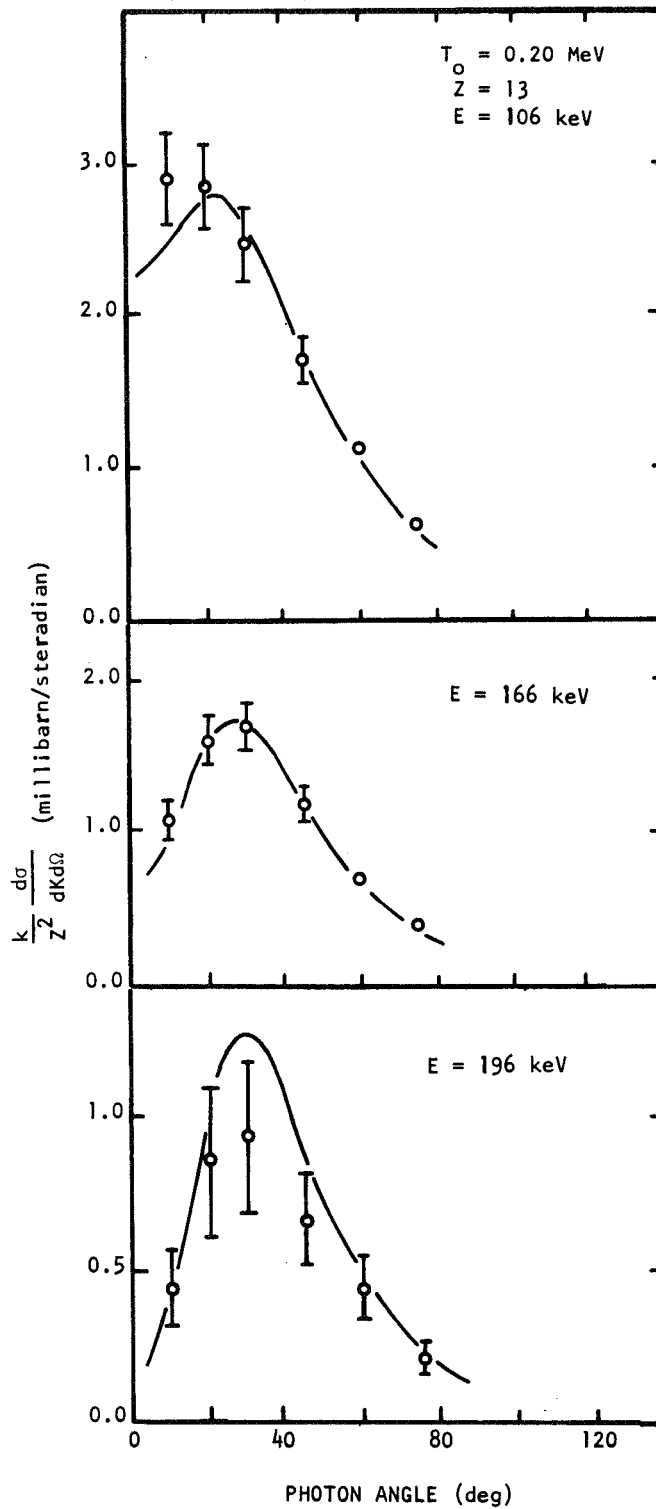


FIGURE 46. BREMSSTRAHLUNG CROSS SECTION VALUES FROM THE WORK OF BRYSK, ET AL. EXPERIMENTAL VALUES ARE SHOWN AS POINTS.

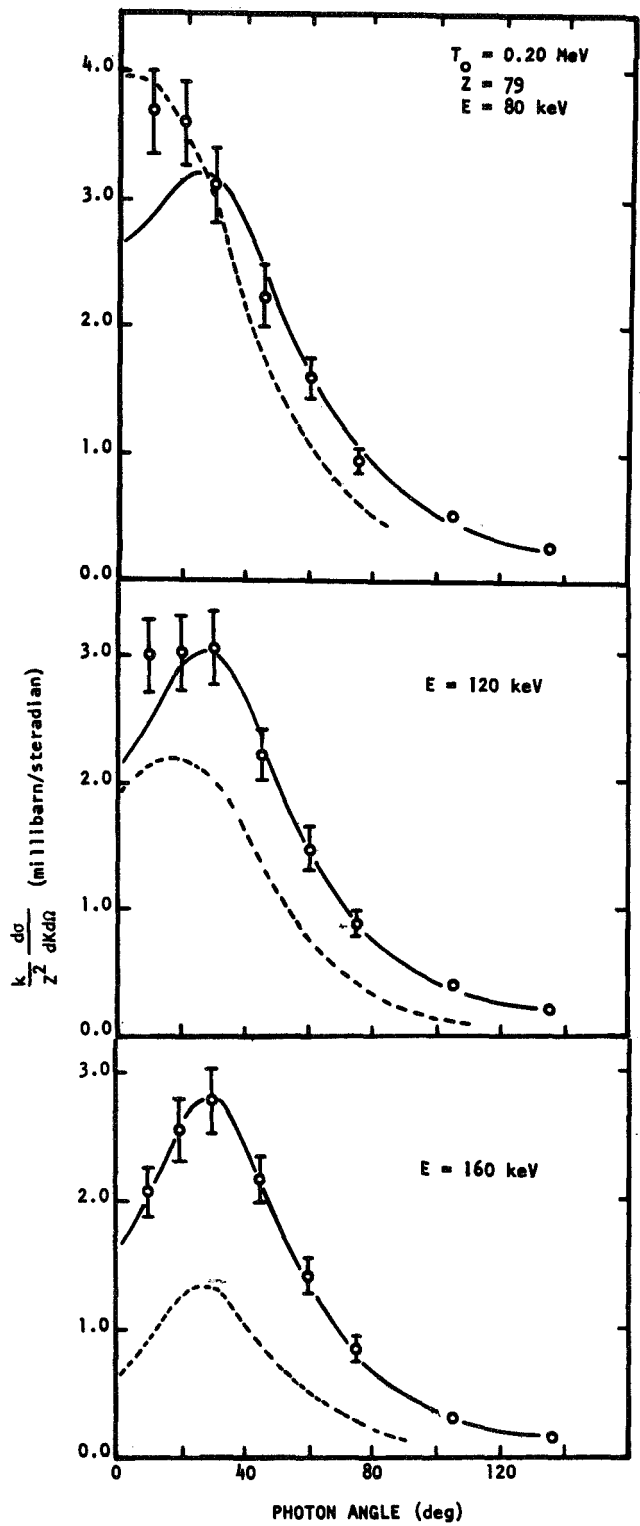


FIGURE 47. BREMSSTRAHLUNG CROSS SECTION VALUES FROM THE WORK OF BRYSK, ET AL (SOLID LINES) AND THE BORN-APPROX. (DASHED LINES). EXPERIMENTAL VALUES ARE SHOWN AS POINTS.

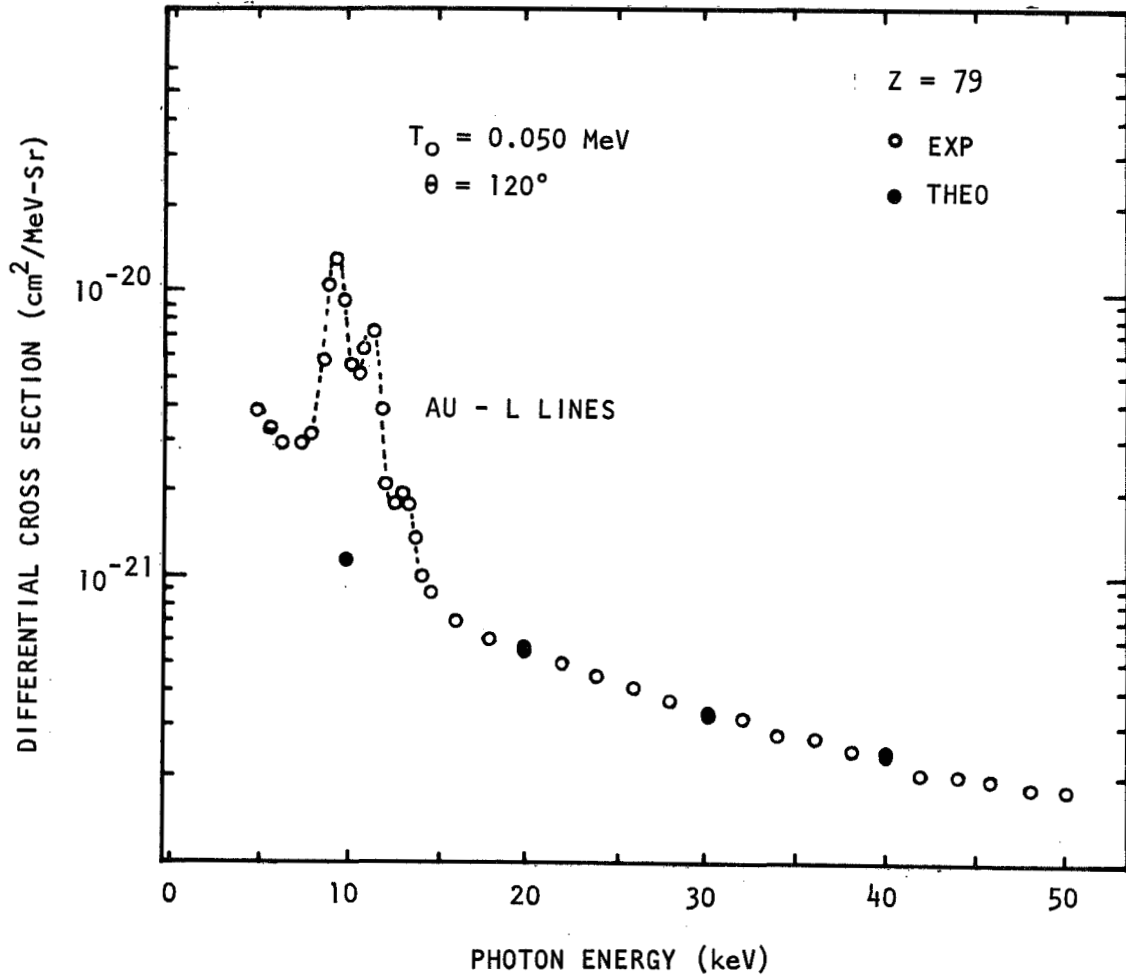


FIGURE 48. BREMSSTRAHLUNG CROSS SECTION VALUES AT 120 DEG. THE THEORETICAL VALUES ARE SHOWN AT PHOTON ENERGIES OF 10, 20, 30, and 40 keV.